$\mathcal{O}(\alpha_s^2)$ corrections to fully-differential top quark decays

Mathias Brucherseifer,[1] **Fabrizio Caola**[2] **and Kirill Melnikov**[2]

[1]*Institut für Theoretische Teilchenphysik, Karlsruhe Institute of Technology (KIT), Germany*

[2]*Department of Physics and Astronomy, Johns Hopkins University, Baltimore, USA*

E-mail: mathias.brucherseifer@kit.edu, caola@pha.jhu.edu, melnikov@pha.jhu.edu

ABSTRACT: We describe a calculation of the fully-differential decay rate of a top quark to a massless *b*-quark and a lepton pair at next-to-next-to-leading order in perturbative QCD. Technical details of the calculation are discussed and selected results for kinematic distributions are shown.

Contents

1 Introduction

Top quark physics at the LHC is benefiting from huge samples of events that can be used to systematically explore many interesting properties of the top quark such as its mass, its production cross-section and the structure of its couplings to other Standard Model particles, including the Higgs boson. Many of such studies require a good understanding of the kinematics of top quark decay products that are affected by QCD radiative corrections.

The next-to-leading (NLO) QCD corrections to the top quark total decay width and many kinematic distributions are known since long ago [1–3]. The electroweak corrections have been computed in Refs. [4]. The fully differential computation of corrections to the top quark width at next-to-leading order was reported in recent years in Refs. [5–7]; it was performed in the context of NLO QCD calculations for a number of processes in top quark physics where radiative corrections to the production and decay stages are incorporated consistently [5–11].

While the NLO QCD description of many hadron collider processes provides quite a reasonable approximation, for some processes it may be useful to improve on that and compute the next-to-next-to-leading order (NNLO) QCD corrections. Top quark pair production in hadron collisions is one of such processes and computations of NNLO QCD corrections to $pp \to t\bar{t}$ are well underway [12–14]. So far these calculations are performed for stable top quarks and address the total cross-section but, eventually, they will mature enough to include also top quark decays in the narrow width approximation. This approximation, when done consistently, includes radiative corrections to production and decay stages and gives an excellent description of the process $pp \to W^+W^-b\bar{b}$ at NLO QCD [15, 16], as was shown explicitly in Ref. [17]. There is no doubt that the narrow width approximation will work very well also at next-to-next-to-leading order, once all relevant corrections

to the production and decay stages are accounted for at a fully-differential level. The goal of this paper is to provide a fully-differential NNLO QCD calculation for the top quark width.

The NNLO QCD radiative corrections to the total width of the top quark were computed in a number of papers [18–21] and, more recently, NNLO QCD corrections to W-helicity fractions were reported in Ref. [22]. However, NNLO QCD corrections to other kinematic distributions in top decays were unknown. We note that very recently NNLO QCD radiative corrections to top quark decay at a fully differential level were computed in Ref. [23], using a slicing method inspired by soft-collinear effective theory [24]. Our computation employs a totally different method and, as such, is complementary to Ref. [23].

A different phenomenological motivation for this computation comes from a similarity between two processes, $t \to b + e^+ + \nu$ and $b \to u + e^- + \bar{\nu}$. This similarity implies that if NNLO QCD radiative corrections are known for an arbitrary invariant mass of the lepton pair, i.e. beyond the narrow W-width approximation, they can be immediately applied to the calculation of NNLO QCD corrections to moments of kinematic distributions in the $b \to u$ semileptonic transition. Since the $b \to u$ decay suffers from significant background from $b \to c$ transition, the inclusive rate for $b \to u$ is of little help for improving the precision with which the CKM matrix element $|V_{ub}|$ can be extracted from experimental measurements. On the other hand, the knowledge of radiative corrections to moments of kinematic distributions with cuts on the electron energy and hadronic invariant mass is useful for constructing a theoretical framework to extract $|V_{ub}|$, see e.g. Refs. [25–28]. The computational framework that we develop in the current paper is immediately applicable to the calculation of these moments.

The other goal of this paper is to contribute to the development of a robust computational scheme that will be applicable to any collider process at NNLO QCD. A promising way towards such a general scheme was described by Czakon [29, 30] who suggested to combine ideas of sector decomposition [31–33] and the Frixione-Kunszt-Signer (FKS) phase-space partitioning [34]. This computational scheme was further discussed in Ref. [35] where it was applied to the calculation of NNLO QED corrections to $Z \to e^+ e^-$. In this paper, we employ these methods to compute NNLO QCD radiative corrections to top quark decay. From the methodological point of view, top quark decay $t \to b + e^+ + \nu$ provides an interesting case where the structure of soft and collinear singularities is relatively simple, yet a massive colored particle in the initial state leads to a computational complexity.

The paper is organized as follows. In the next Section, we discuss the general set up of the computation. In Section 3 we explain how the phase-space for various subprocesses related to top quark decays can be parametrized to enable the extraction of infra-red and collinear singularities. In Section 4 we discuss the singular limits of various amplitudes required for our computation. In Section 5 we explain some peculiarities that arise when we try to keep all momenta of external particles in four dimensions, yet use dimensional regularization consistently. In Section 6 we describe the results of the calculation and show some kinematic distributions. In Section 7 we present our conclusions. Finally, we give explicit expressions for tree amplitudes employed in our calculation in Appendix A and show how to compute one-loop master integrals needed in the constructions of one-loop soft limits in Appendix B.

2 The set up

As we already mentioned in the Introduction, our goal in this paper is to compute NNLO QCD corrections to the fully differential decay rate of the top quark $t(p_t) \longrightarrow b(p_b) + \nu_e(p_5) + e^+(p_6)$. Throughout the paper, we work in the top quark rest frame. The decay to $e^+ \nu$ is facilitated by an emission of a W-boson, which can be either on or off the mass-shell. The interaction of the virtual W

boson with the neutrino-positron pair $W \to \nu(p_5) + e^+(p_6)$ is described by the vertex

$$\frac{ig_W}{\sqrt{2}} \langle 5|\gamma^\mu|6], \tag{2.1}$$

where we use the bra and ket notation for massless spinors with definite helicities. We employ the standard notation $u_+(p_i) = |p_i, +\rangle = |i\rangle$, $u_-(p_i) = |p_i, -\rangle = |i]$ and note that further discussion of spinor-helicity methods can be found in the review Ref. [36].

We are interested in the NNLO QCD corrections to semileptonic top quark decay. To compute these radiative corrections, we require the following ingredients

- two-loop virtual corrections to $t \to b + \nu + e^+$;

- one-loop virtual corrections to $t \to b + g + \nu + e^+$;

- tree-level double-real emission contributions to the decay rate, $t \to b + g + g + \nu + e^+$ and $t \to b + q\bar{q} + \nu + e^+$.

We note that most of the required contributions are available in the literature. Indeed, two-loop QCD virtual corrections to $t \to Wb$ can be obtained from an analytic computation of similar corrections to $b \to W^*u$, reported recently by a number of authors [37–41]. One-loop amplitudes for the $t \to b + g + \nu + e^+$ process can be extracted from Ref. [6]. Double-real emission amplitudes for gluons and quarks are not known in a compact analytic form but can be easily calculated using the spinor-helicity formalism.

However, similar to other NNLO computations, the availability of required amplitudes does not make it obvious how to arrive at a physical answer. This happens because of infra-red and collinear singularities that need to be extracted from individual contributions before integrating over phase-spaces of final-state particles. Until recently, the two methods[1] that were used to extract singularities in practical NNLO computations were sector decomposition [31–33] and antenna subtraction [46, 47]. Both of these methods were developed further in recent years [48, 49] with the goal to make them applicable to more complex processes than previously considered.

The method that we use in this paper was suggested by Czakon [29, 30] (see also [35]), who pointed out that a combination of sector decomposition [31–33] and the FKS phase-space partitioning [34] allows to resolve overlapping soft and collinear singularities in a universal way. We note that from the technical point of view, the case of top quark decay is particularly simple since no complicated phase-space partitioning is, in fact, required. Indeed, singularities in matrix elements occur when emitted gluons are either soft or collinear to other massless partons. Since there are only three strongly interacting massless particles in double-real emission amplitudes for top decays, there is just one triple-collinear limit and no need for angular partitioning arises. The soft singularities are disentangled by ordering gluons with respect to their energies and by removing the corresponding $1/2!$ factor from the phase-space. Note that this argument needs to be modified for sub-processes with two quarks in the final state and we explain how to do it in what follows.

We now remind the reader about the general approach to fully differential NNLO QCD computations based on sector decomposition and phase-space partitioning [29, 30] (see also [35]). The main idea is to express the phase-space for the final state particles through suitable unit-hypercube variables that make the singular behavior of scattering amplitudes manifest. Once this is accomplished, it is easy

---

[1]Other approaches to NNLO calculations are discussed in [42–44]. Some phenomenological applications can be found in [45].

to construct subtraction terms for real emission processes by using expansion in plus-distributions. To be specific, we consider a double-real emission contribution to the differential decay rate of the top quark

$$\Gamma_t^{(RR)} = \int \mathrm{dLips} \ |\mathcal{M}(\{p\})|^2 J(\{p\}), \tag{2.2}$$

where dLips is a phase-space for $t \to b + g + g + e^+ + \nu$, $\mathcal{M}(\{p\})$ is the decay amplitude and $J(\{p\})$ is a measurement function that depends on momenta of final state particles $\{p\}$. We assume that a map of the phase-space onto a unit hypercube is found; variables that parametrize the map are denoted as $\{x\}$. As we will show below, it is possible to re-write Eq.(2.2) as

$$\Gamma_t^{(RR)} = \sum_{i=1}^{N_S} \Gamma_t^{(RR,i)}, \quad \Gamma_t^{(RR,i)} = \prod_{j=1}^{N_{\mathrm{ps}}} \int_0^1 \frac{\mathrm{d}x_j}{x_j^{1+a_j^{(i)}\epsilon}} F_i(\epsilon, \{x\}) \tag{2.3}$$

where N_S is the number of sectors, $\epsilon = (4-d)/2$ is the parameter of dimensional regularization, N_{ps} is the number of independent variables required to parametrize the phase-space, and the function F is the product of the scattering amplitude squared, sector-dependent powers of singular variables and the phase-space weight $\mathrm{Ps}_w(\{x\})$ that may include the measurement function

$$F_i(\{x\}) = x_1^{b_1} x_2^{b_2} .. x_{N_{ps}}^{b_{N_{ps}}} |\mathcal{M}(\{p\})|^2 \ \mathrm{Ps}_w(\{x\}). \tag{2.4}$$

The important property of these functions F_i is that limits exist at each potentially singular point $x_j = 0$,

$$\lim_{x_j=0} F_i(.., x_j, ..) = F_i(.., 0, ..) \neq \infty. \tag{2.5}$$

The existence of limits Eq.(2.5) allows us to re-write Eq.(2.3) in an explicitly integrable form by employing the decomposition in plus-distributions

$$\frac{1}{x^{1+a\epsilon}} = -\frac{1}{a\epsilon}\delta(x) + \sum_{n=0}^{\infty} \frac{(-\epsilon a)^n}{n!} \left[\frac{\ln^n(x)}{x}\right]_+ . \tag{2.6}$$

Substituting this expansion into Eq.(2.3) and collecting terms of the same order in ϵ, we obtain explicitly integrable terms that can be divided into two broad categories,

$$\int_0^1 \mathrm{d}x_i \ \frac{\ln^n(x_i) \left(F(.., x_i, ..) - F(.., 0, ..)\right)}{x_i} \quad \text{and} \quad \int_0^1 \mathrm{d}x_i \delta(x_i) F(.., 0, ..). \tag{2.7}$$

It is easy to recognize that the first integral in the above equation contains a "subtraction term" and the second integral defines an "integrated subtraction term", if the language familiar from NLO QCD computations is borrowed. It is remarkable that, in the described framework, the subtraction terms are obtained automatically, once a proper parametrization of the phase-space is found and the expansion in plus-distributions is performed. We also note that any subtraction term depends on the function $F(x_1, .., x_{N_{ps}})$ at such values of x_i for which at least one of the singular variables vanishes. These kinematic points correspond to *universal soft and collinear limits* of scattering amplitudes so that $F(.., x_i = 0, ..)$ can be calculated in a process-independent way. In what follows, we discuss essential elements of this construction such as the phase-space parametrization and singular limits of amplitudes.

Before proceeding to that discussion, we explain some subtleties that arise when *one-loop* corrections to the process $t \to b + g + e^+ + \nu$ are analyzed within this framework. In this case, the singular part of the phase-space is parametrized in terms of two variables, x_1 and x_2, that describe the energy of the gluon g and the relative angle between the gluon and the b-quark, respectively. The contribution to the top quark decay rate is given by the integral

$$\int\limits_0^1 \frac{\mathrm{d}x_1}{x_1^{1+2\epsilon}} \frac{\mathrm{d}x_2}{x_2^{1+\epsilon}} \, [x_1^2 x_2] 2\mathrm{Re} \left[\mathcal{M}_{t\to bge^+\nu}^{1-\mathrm{loop}} \mathcal{M}_{t\to bge^+\nu}^{(0),*} \right] ..., \tag{2.8}$$

where ellipses stand for other non-singular phase-space factors. While the integrand in Eq.(2.8) suggests that singularities can be isolated by constructing an expansion in plus-distributions, it is in fact not possible to do that right away. The reason is that the one-loop amplitude $\mathcal{M}_{t\to bge^+\nu}^{1-\mathrm{loop}}$ has *branch cuts* in the limits $x_1 \to 0$ and $x_2 \to 0$ and we must account for them when constructing the expansion of the integrand in plus-distributions. To accomplish that, we write

$$[x_1^2 x_2] \left[\mathcal{M}_{t\to bge^+\nu}^{1-\mathrm{loop}} \mathcal{M}_{t\to bge^+\nu}^{(0),*} \right] \sim F_1(x_1, x_2, ..) + (x_1^2 x_2)^{-\epsilon} F_2(x_1, x_2, ..), \tag{2.9}$$

where the two functions $F_{1,2}$ are *free* from branch cuts in $x_{1,2} \to 0$ limits.

The calculation of real-virtual corrections now proceeds as follows. We insert Eq.(2.9) into Eq.(2.8), combine non-integer powers of $x_{1,2}$ and expand in plus-distributions. Upon doing so, we find a variety of terms that are similar to what we showed in Eq.(2.7). However, in this case the integrand is written in terms of $F_1(x_1, x_2)$ and $F_2(x_1, x_2)$ and we need a prescription that will allow us to compute these functions from scattering amplitudes. To understand how this is done, note that $F_{1,2}(\{x\})$ may appear in the integrand with one or both of its arguments set to zero, which corresponds to soft or collinear kinematics of the final state gluon. To compute $F_{1,2}$ in those cases, we need to investigate $\left[\mathcal{M}_{t\to bge^+\nu}^{1-\mathrm{loop}} \mathcal{M}_{t\to bge^+\nu}^{(0),*} \right]$ in soft and collinear limits. Consider first the soft limit, $x_1 \to 0$. In this case, the interference of the one-loop and tree matrix elements reads

$$\lim_{x_1\to 0} 2\mathrm{Re} \left[\mathcal{M}_{t\to bge^+\nu}^{1-\mathrm{loop}} \mathcal{M}_{t\to bge^+\nu}^{(0),*} \right] = g_s^2 C_F S_{tb} \left(2\mathrm{Re} \left[\mathcal{M}_{t\to be^+\nu}^{1-\mathrm{loop}} \mathcal{M}_{t\to be^+\nu}^{(0),*} \right] \right) \\ + g_s^2 C_A S_{tb}^{(1)} \left[\mathcal{M}_{t\to be^+\nu}^{(0)} \mathcal{M}_{t\to be^+\nu}^{(0),*} \right], \tag{2.10}$$

where S_{tb} and $S_{tb}^{(1)}$ are tree and one-loop eikonal factors, respectively. We note that in the right hand side of Eq.(2.10), the dependence of the one-loop amplitude on the momentum of the soft gluon is entirely contained in the eikonal factors. To identify $F_{1,2}$ at vanishing value of x_1, it is important to realize that the leading-order eikonal factor S_{tb} is free from branch cuts while the one-loop eikonal factor $S_{tb}^{(1)}$ may (and in fact does) contain them. We conclude that, in the soft limit $x_1 \to 0$, the first term on the right hand side in Eq.(2.10) matches to $F_1(0, x_2)$ and the second term to $F_2(x_1 = 0, x_2)(x_1^2 x_2)^{-\epsilon}$.

A similar situation occurs in the collinear limit $x_2 \to 0$. In this case

$$\lim_{x_2\to 0} \left[\mathcal{M}_{t\to bge^+\nu}^{1-\mathrm{loop}} \mathcal{M}_{t\to bge^+\nu}^{(0),*} \right] = \frac{g_s^2}{p_b \cdot p_g} \left(P_{b\to bg}^{(0)} \left[\mathcal{M}_{t\to \tilde{b}e^+\nu}^{1-\mathrm{loop}} \mathcal{M}_{t\to \tilde{b}e^+\nu}^{(0),*} \right] + P_{b\to bg}^{(1)} \left[\mathcal{M}_{t\to \tilde{b}e^+\nu}^{(0)} \mathcal{M}_{t\to \tilde{b}e^+\nu}^{(0),*} \right] \right), \tag{2.11}$$

where $P_{b\to bg}^{(0,1)}$ are the tree- and one-loop splitting functions; these functions can be derived from collinear limits of scattering amplitudes described in Ref. [50]. Similar to the soft limit, the tree-level splitting function $P_{b\to bg}^{(0)}$ does not contain any branch cut in $x_2 \to 0$ limit, while the one-loop splitting function

does. Hence, the first term on the right-hand side in Eq.(2.11) is identified with $F_1(x_1, x_2 = 0)$ and the second one with $(x_1^2 x_2)^{-\epsilon} F_2(x_1, x_2 = 0)$.

If x_1 and x_2 are *both* non-vanishing, we can re-write combinations of $F_1(x_1, x_2)$ and $F_2(x_1, x_2)$ that appear in the integrand for the rate, through the one-loop matrix element interfered with the tree-level amplitude, using Eq.(2.9). The one-loop amplitude for the $t \to b + g + e^+ + \nu$ that we require, can be extracted from Ref. [6], where Wt production in bg fusion is discussed.[2] For our purpose, the relevant amplitudes need to be crossed to describe the $t \to b + g + W^+$ channel. Finally, the evaluation of the one-loop amplitude for $t \to b + g + e^+ + \nu$ process requires master integrals; they can be computed using the program QCDLoops [52]. We found, however, that results of this program become unreliable in extreme kinematic limits; for example when the momentum of the gluon in the final state becomes very small $E_g \lesssim 10^{-8} m_t$. To overcome this difficulty, we independently implemented all master integrals relevant for the computation of the one-loop amplitude for $t \to b + g + e^+ + \nu$ using analytic formulas provided in Refs. [52, 53]. Our implementation allows us to employ quadruple precision and to reach very small gluon energies $E_g \sim 10^{-12} m_t$ and very small opening angles between the bottom quark and the gluon.

The importance of reaching small energies and angles follows from Eq.(2.7) which shows that integration over hypercube variables $\{x\}$ should, in principle, be performed on the interval $x_i \in [0, 1]$. This implies that full matrix elements that contribute to the function $F(x)$ must be evaluated at vanishingly small values of x. It is, of course, impossible to compute them at $x = 0$ and we need to introduce additional regularization. Following Refs. [29, 30] we provide this regularization by discarding such points in $\{x\}$-space where the product of singular variables is smaller than a user-defined parameter δ. For example, for double-real emission corrections where four variables are singular, we require $x_1 x_2 x_3 x_4 > \delta$, while for the single-emission contributions we require $x_1 x_2 > \delta$. Values of δ that we use range from 10^{-7} to 10^{-12}, where extremely small values are employed to test the independence of final results on the cut-off parameter and the cancellation of infra-red divergences. For phenomenological calculations we find that values of $\delta \sim 10^{-7} - 10^{-9}$ are small enough to provide reasonable results for the second order corrections.

Finally, we note that Eq.(2.7) allows us to compute arbitrary kinematic distributions in a single run of the code. We only need to determine the kinematics of the event – which is uniquely defined for a given set of $\{x\}$-variables – and assign the relevant weight to a particular bin in a histogram that we want to compute. We do this each time the function $F(\{x\})$ is calculated. Such implementation is standard for how subtraction procedure is employed in parton level Monte-Carlo event generators both at next-to-leading order (see e.g. Ref. [51]) and beyond [54].

3   Phase-spaces for various sub-processes in top decays

In this Section, we discuss the phase-space parametrization for the various sub-processes related to top quark decays. We start with the leading order phase-space and then proceed to phase-spaces with one and two additional gluons in the final state. We also address the parametrization of the phase-space for $t \to b + q\bar{q} + e^+ + \nu$ since it differs from the two-gluon case in important details.

The *leading order process* that we deal with is $t \to b + W^*(e^+ + \nu)$, where the W-boson can be off the mass shell. While the W off-shellness is not an important effect for top quark decays, our reasons for doing the calculation this way is explained in the Introduction. To account for the W

---

[2] We use the Fortran77 implementation of this amplitude in the MCFM program [51]. We slightly extend it to allow the use of quadruple precision in Fortran90.

off-shellness in a systematic way, it is convenient to include the Breit-Wigner propagator from the scattering amplitude into the definition of the phase-space. We write

$$d\Pi_{be^+\nu} = \frac{dp_W^2}{2\pi} \frac{\text{Lips}(t \to bW^*)d\text{Lips}(W^* \to \nu l^+)}{(p_W^2 - m_W^2)^2 + m_W^2 \Gamma_W^2}, \tag{3.1}$$

where Lips stands for Lorentz-invariant phase-spaces for indicated final states, p_W^2 is the invariant mass of the lepton pair and Γ_W is the W-decay width. We remove the Breit-Wigner distribution by changing variables

$$p_W^2 = m_W^2 + m_W \Gamma_W \tan \xi, \tag{3.2}$$

so that

$$\frac{1}{2\pi} \frac{dp_W^2}{(p_W^2 - m_W^2)^2 + m_W^2 \Gamma_W^2} = \frac{d\xi}{2\pi m_W \Gamma_W}. \tag{3.3}$$

The kinematics of the process implies a restriction on the invariant mass of the lepton pair, $0 < p_W^2 < m_t^2$. To account for it, we re-map ξ onto the $(0,1)$ interval by defining $\xi = \xi_{\min} + (\xi_{\max} - \xi_{\min})x_7$. We obtain

$$\frac{1}{2\pi} \frac{dp_W^2}{(p_W^2 - m_W^2)^2 + m_W^2 \Gamma_W^2} = N_{\text{BW}} \, dx_7, \tag{3.4}$$

where

$$N_{\text{BW}} = \frac{\xi_{\max} - \xi_{\min}}{2\pi m_W \Gamma_W}, \quad \xi_{\min} = -\arctan \frac{m_W}{\Gamma_W}, \quad \xi_{\max} = \arctan \left[\frac{m_t^2 - m_W^2}{m_W \Gamma_W} \right]. \tag{3.5}$$

After generating the invariant mass of the lepton pair using Eq.(3.4) , we obtain lepton and neutrino momenta in the W^* rest frame in the standard way

$$p_{\nu,l} = \frac{\sqrt{p_W^2}}{2}(1, \pm \vec{n}_l), \tag{3.6}$$

where $\vec{n}_l = (\sin\theta_5 \cos\varphi_5, \sin\theta_5 \sin\varphi_5, \cos\theta_5)$. Redefining angular variables,

$$\cos\theta_5 = 1 - 2x_8, \qquad \varphi_5 = 2\pi x_9, \tag{3.7}$$

we re-write the dilepton phase-space as

$$d\text{Lips}(W^* \to \nu l^+) = \frac{dx_8 dx_9}{8\pi}. \tag{3.8}$$

We note that we treat the lepton-neutrino phase-space as four-dimensional, even in higher orders of QCD perturbation theory where infra-red and collinear divergences require analytic continuation of the space-time dimensionality. It is intuitively clear that it should be possible to do so because lepton momenta are infra-red safe observables. However, some subtleties arise when the computation is organized this way. We discuss them in Section 5.

Finally, we describe the parametrization of the $t \to bW^*$ phase-space. We work in the rest frame of the decaying top quark and define the z-axis by aligning it with the momentum of the b-quark. The momenta read

$$p_t = m_t(1, 0, 0, 0), \quad p_b = E_b(1, \vec{n}_b), \quad \vec{n}_b = (0, 0, 1). \tag{3.9}$$

The energy of the b-quark is given by

$$E_b = \frac{m_t^2 - p_W^2}{2m_t}. \tag{3.10}$$

It is easy to find the leading order phase-space for $t \to bW^*$ decay. It reads

$$\text{Lips}(t \to bW) = \frac{1}{8\pi} \left(1 - \frac{p_W^2}{m_t^2} \right) \Upsilon(\epsilon) = \frac{E_{\text{max}}}{4\pi m_t} \Upsilon(\epsilon), \tag{3.11}$$

where $E_{\text{max}} = E_b$ is the maximal energy of the b-quark for fixed invariant mass of the lepton pair and

$$\Upsilon(\epsilon) = \frac{\Gamma(1-\epsilon)}{\Gamma(2-2\epsilon)} \left(\frac{E_{\text{max}}^2}{\pi} \right)^{-\epsilon} = 1 + \mathcal{O}(\epsilon). \tag{3.12}$$

We can then write the leading order phase-space for $t \to b + e^+ + \nu$ as

$$\text{d}\Pi_{be^+\nu} = \Upsilon(\epsilon) N_{\text{BW}} \frac{E_{\text{max}}}{32\pi^2 m_t} \text{d}x_7 \text{d}x_8 \text{d}x_9 = \frac{\Upsilon(\epsilon) N_{\text{BW}}}{64\pi^2} \left(1 - \frac{p_W^2}{m_t^2} \right) \text{d}x_7 \text{d}x_8 \text{d}x_9. \tag{3.13}$$

The ϵ-dependent part of the leading order phase-space $\Upsilon(\epsilon)$ can be neglected provided that *exactly* the same quantity is identified and removed from phase-spaces in higher orders of perturbation theory. In our calculation, we set $\Upsilon(\epsilon) = 1$ consistently everywhere.

We now turn to the phase-space which is relevant for the description of the single emission process $t \to b + g(p_3) + e^+ + \nu$. The treatment of the W^* decay phase-space and the Breit-Wigner factor is identical to the leading order case; the new element is the phase-space for the process $t \to W^* + b + g$, which we refer to as $\text{dLips}(t \to bgW^*)$. This phase-space is split into "regular" and "singular" parts

$$\text{dLips}(t \to bgW^*) = \text{dLips}(Q \to bW^*) \times [\text{d}p_3], \tag{3.14}$$

where $Q = p_t - p_3$, $[\text{d}p_3] = \text{d}^{D-1} p_3 / [(2\pi)^{D-1} 2E_3]$ and

$$\text{dLips}(Q \to bW^*) = (2\pi)^D \delta^{(D)}(Q - p_b - p_W)[\text{d}p_b][\text{d}p_W]. \tag{3.15}$$

The momenta that enter the "regular" phase-space read

$$p_t = m_t(1,0,0,0), \quad p_b = E_b(1,\vec{n}_b), \quad E_b = \frac{Q^2 - p_W^2}{2(Q_0 - \vec{Q}\cdot\vec{n}_b)}. \tag{3.16}$$

We find

$$\text{dLips}(Q \to bW^*) = \frac{\Upsilon(\epsilon)}{4\pi} \frac{E_b}{Q_0 - \vec{Q}\cdot\vec{n}_b} \left(\frac{E_b}{E_{\text{max}}} \right)^{-2\epsilon}. \tag{3.17}$$

The gluon momentum is parametrized as

$$p_3 = E_3(1, \sin\theta_3 \cos\varphi_3, \sin\theta_3 \sin\varphi_3, \cos\theta_3), \tag{3.18}$$

where gluon energy and emission angles are computed from unit hypercube variables

$$E_3 = x_1 E_{\text{max}}, \quad \cos\theta_3 = 1 - 2x_2, \quad \varphi_3 = 2\pi x_3. \tag{3.19}$$

Expressed through these variables, the singular phase-space becomes

$$[\text{d}p_3] = \frac{\Gamma(1-\epsilon)\text{PS}^{-\epsilon}}{8\pi^2(4\pi)^{-\epsilon}\Gamma(1-2\epsilon)} 2E_{\text{max}}^2 \frac{\text{d}x_1 \text{d}x_2 \text{d}x_3}{x_1^{1+2\epsilon} x_2^{1+\epsilon}} \left[x_1^2 x_2 \right], \tag{3.20}$$

where $\text{PS} = 16 E_{\text{max}}^2 (1 - x_2) \sin^2\varphi_3$. We note that the term $[x_1^2 x_2]$ in Eq.(3.20) gets combined with the matrix element squared $|\mathcal{M}_{t \to b + e^+ + \nu + g}|^2$ to render the function $F(x)$, that we discussed in the

previous Section. It is this factor from the phase-space that makes $F(x)$ finite both in the soft $x_1 \to 0$ and in the collinear $x_2 \to 0$ limits. We find it convenient to factor out a term $\Gamma(1+\epsilon)/[8\pi^2(4\pi)^{-\epsilon}]$ per order in perturbation theory and to write the final result for the differential top quark width as a series in $\alpha_s/(2\pi)$. We therefore write the phase-space for the process $t \to b + g(p_3) + e^+ + \nu$ as

$$
\begin{aligned}
\mathrm{d}\Pi_{bge^+\nu} &= \Upsilon(\epsilon)\frac{\Gamma(1+\epsilon)}{8\pi^2(4\pi)^{-\epsilon}}N_{\mathrm{BW}}\left(\frac{\Gamma(1-\epsilon)}{\Gamma(1+\epsilon)\Gamma(1-2\epsilon)}\right) \\
&\times \frac{E_{\max}^2}{16\pi^2}\frac{E_b}{Q_0 - \vec{Q}\cdot\vec{n}_b}\left(\frac{E_b}{E_{max}}\right)^{-2\epsilon}\mathrm{PS}^{-\epsilon}\frac{\mathrm{d}x_1}{x_1^{1+2\epsilon}}\frac{\mathrm{d}x_2}{x_2^{1+\epsilon}}\,\mathrm{d}x_3\mathrm{d}x_7\mathrm{d}x_8\mathrm{d}x_9\,[x_1^2x_2],
\end{aligned}
\tag{3.21}
$$

where $Q = p_t - p_3$.

Finally, we discuss the phase-space for the *double-real emission process* $t \to b + g(p_3) + g(p_4) + e^+ + \nu$. Similar to the single-gluon case that we just discussed, the phase-space is split into a regular and a singular part. The regular phase-space is identical to the single gluon emission case Eq.(3.17), up to a change in the definition of the momentum $Q = p_t - p_3 - p_4$. The singular phase-space is given by the product of single-particle phase-spaces of the two gluons, $g(p_3)$ and $g(p_4)$. We choose the momenta to be

$$
\begin{aligned}
p_t &= m_t(1,0,0,0), \quad p_b = E_b(1,\vec{n}_b), \quad p_3 = E_3(1,\vec{n}_3), \quad p_4 = E_4(1,\vec{n}_4), \\
\vec{n}_3 &= (\sin\theta_3\cos\varphi_3, \sin\theta_3\sin\varphi_3, \cos\theta_3), \quad \vec{n}_4 = (\sin\theta_4\cos\varphi_{34}, \sin\theta_4\sin\varphi_{34}, \cos\theta_4),
\end{aligned}
\tag{3.22}
$$

with $\varphi_{34} = \varphi_3 + \varphi_4$. We compute the azimuthal angle φ_3 using $\varphi_3 = 2\pi x_6$. We note that the number of particles that participate in the "QCD part" of the process is sufficiently small, so that we can embed momenta of top and bottom quarks and of the two gluons into a four-dimensional space-time. By momentum conservation, the momentum of the W-boson is also four-dimensional, but this does not imply that momenta of a lepton and a neutrino can be chosen to be four-dimensional as well. We will argue in Section 5 that it is in fact possible to do that provided that *a spin-correlation part of certain splitting functions is modified.*

The correct choice of phase-space variables is crucial for extracting singularities from products of matrix elements squared and phase-space factors. For the two-gluon case, we must consider the following singular limits: *i)* one or both gluons are soft; *ii)* one or both gluons are collinear to a b-quark and *iii)* two gluons are collinear to each other. The parametrization of phase-space that leads to factorization of these singularities was given in Refs. [29, 30] and we now discuss it in the context of top quark decay. We note that by ordering two gluons in energy, we remove the 2! symmetry factor from the phase-space. We write the singular phase-space as

$$
\begin{aligned}
[\mathrm{d}p_3][\mathrm{d}p_4]\theta(E_3 - E_4) &= \frac{\mathrm{d}\Omega^{(d-3)}\mathrm{d}\Omega^{(d-3)}}{2^{5+2\epsilon}(2\pi)^{2d-2}}\mathrm{d}\varphi_3\left[\sin^2(\varphi_3)\right]^{-\epsilon} \\
&\times [\xi_1\xi_2]^{1-2\epsilon}\left[\eta_3(1-\eta_3)\right]^{-\epsilon}\left[\eta_4(1-\eta_4)\right]^{-\epsilon}\left[\lambda(1-\lambda)\right]^{-1/2-\epsilon}\frac{|\eta_3 - \eta_4|^{1-2\epsilon}}{D^{1-2\epsilon}} \\
&\times (2E_{\max})^{4-4\epsilon}\,\theta(\xi_1 - \xi_2)\theta\left(x_{\max} - \xi_2\right)\,\mathrm{d}\xi_1\mathrm{d}\xi_2\mathrm{d}\eta_3\mathrm{d}\eta_4\mathrm{d}\lambda.
\end{aligned}
\tag{3.23}
$$

Various variables introduced in the above formula parametrize energies and angles of the (potentially) unresolved gluons. We use

$$
E_{3,4} = E_{\max}\xi_{1,2}, \qquad x_{\max} = \min\left[1, \frac{1-\xi_1}{\xi_1(1-(1-p_W^2/m_t^2)\xi_1\eta_{34})}\right],
\tag{3.24}
$$

and

$$\eta_{34} = \frac{|\eta_3 - \eta_4|^2}{D(\eta_3, \eta_4, \lambda)}, \quad \sin^2 \varphi_4 = 4\lambda(1-\lambda) \frac{|\eta_3 - \eta_4|^2}{D(\eta_3, \eta_4, \lambda)^2},$$
$$D(\eta_3, \eta_4, \lambda) = \eta_3 + \eta_4 - 2\eta_3\eta_4 + 2(2\lambda - 1)\sqrt{\eta_3\eta_4(1-\eta_3)(1-\eta_4)}. \quad (3.25)$$

The η-variables are defined as the following scalar products

$$2\eta_{3,4} = 1 - \vec{n}_{3,4} \cdot \vec{n}_b, \quad 2\eta_{34} = 1 - \vec{n}_3 \cdot \vec{n}_4. \quad (3.26)$$

Parametrization of the singular phase-space in Eq.(3.23) is still too complicated to extract all singularities; further decomposition is required. This is achieved by a sequence of variable changes that we describe below following Refs. [29, 30]. Specifically, we split the phase-space into a sum of five different sectors. In each of these sectors, the relation between "old" variables $\{\eta, \xi\}$ and "new" variables $\{x\}$ reads

$$\text{sector } 1: \quad \xi_1 = x_1, \ \xi_2 = x_1 x_{\max} x_2, \ \eta_3 = x_3, \ \eta_4 = \frac{x_3 x_4}{2},$$
$$\text{sector } 2: \quad \xi_1 = x_1, \ \xi_2 = x_1 x_{\max} x_2, \ \eta_3 = x_3, \ \eta_4 = x_3 \left(1 - \frac{x_4}{2}\right),$$
$$\text{sector } 3: \quad \xi_1 = x_1, \ \xi_2 = x_1 x_{\max} x_2 x_4, \ \eta_3 = \frac{x_3 x_4}{2}, \ \eta_4 = x_3, \quad (3.27)$$
$$\text{sector } 4: \quad \xi_1 = x_1, \ \xi_2 = x_1 x_{\max} x_2, \ \eta_3 = \frac{x_3 x_4 x_2}{2}, \ \eta_4 = x_3,$$
$$\text{sector } 5: \quad \xi_1 = x_1, \ \xi_2 = x_1 x_{\max} x_2, \ \eta_3 = x_3 \left(1 - \frac{x_4}{2}\right), \ \eta_4 = x_3.$$

We also write $\lambda = \sin^2(\pi x_5/2)$. This change of variables introduces a factor of π in the normalization of the phase-space that is included in the expressions below. The integration region for x_5 is $x_5 \in [0, 1]$.

The full phase-space for $t \to b + g + g + e^+ + \nu$ is given by the sum of five (sector) phase-spaces

$$d\Pi_{bg_3 g_4 e^+ \nu} = \sum_{i=1}^{5} d\Pi_{bg_3 g_4 e^+ \nu}^{(i)}. \quad (3.28)$$

Each of the five phase-spaces is written as

$$d\Pi_{bg_3 g_4 e^+ \nu}^{(i)} = \text{Norm} \times \text{PS}_{w,i} \text{PS}_i^{-\epsilon} \prod_{k=5}^{9} dx_k \times \prod_{j=1}^{4} \frac{dx_j}{x_j^{1+a_j^{(i)}\epsilon}} \times \left[x_1^{b_1^{(i)}} x_2^{b_2^{(i)}} x_3^{b_3^{(i)}} x_4^{b_4^{(i)}} \right]. \quad (3.29)$$

Below we present the functions $\text{PS}_{w,i}$, PS_i and the exponents $a_{j=1...4}^{(i)}$ and $b_{j=1...4}^{(i)}$ for each of the sectors. We note that the normalization factor is common to all sectors; it reads

$$\text{Norm} = \Upsilon(\epsilon) \left[\frac{\Gamma(1+\epsilon)}{(4\pi)^{-\epsilon} 8\pi^2} \right]^2 N_{\text{BW}} \left(\frac{\Gamma(1-\epsilon)}{\Gamma(1+\epsilon)\Gamma(1-2\epsilon)} \right)^2. \quad (3.30)$$

We also note that we can write

$$\text{PS}_{w,i} = \frac{1}{8\pi^2} \frac{E_b E_{\max}^4 x_{\max}^2}{Q_0 - \vec{Q} \cdot \vec{n}_b} \overline{\text{PS}}_{w,i}, \quad \text{PS}_i = 1024 E_b^2 E_{\max}^2 \lambda(1-\lambda) x_{\max}^2 (1-x_3) \sin^2(\varphi_3) \overline{\text{PS}}_i. \quad (3.31)$$

The expressions for the exponents and the phase-space factors for each of the five sectors read[3]

$$\underline{\text{sector } 1}: \quad \{a_1 = 4, a_2 = 2, a_3 = 2, a_4 = 1\}, \quad \{b_1 = 4, b_2 = 2, b_3 = 2, b_4 = 1\},$$

$$\overline{\text{PS}}_w = \frac{\left(1 - \frac{x_4}{2}\right)}{2N_1(x_3, \frac{x_4}{2}, \lambda)}, \quad \overline{\text{PS}} = \frac{\left(1 - \frac{x_3 x_4}{2}\right)\left(1 - \frac{x_4}{2}\right)^2}{2N_1^2(x_3, \frac{x_4}{2}, \lambda)},$$

$$\underline{\text{sector } 2}: \quad \{a_1 = 4, a_2 = 2, a_3 = 2, a_4 = 2\}, \quad \{b_1 = 4, b_2 = 2, b_3 = 2, b_4 = 2\},$$

$$\overline{\text{PS}}_w = \frac{1}{4N_1(x_3, 1 - \frac{x_4}{2}, \lambda)}, \quad \overline{\text{PS}} = \frac{\left(1 - \frac{x_4}{2}\right)\left(1 - x_3(1 - \frac{x_4}{2})\right)}{4N_1^2(x_3, 1 - \frac{x_4}{2}, \lambda)},$$

$$\underline{\text{sector } 3}: \quad \{a_1 = 4, a_2 = 2, a_3 = 2, a_4 = 3\}, \quad \{b_1 = 4, b_2 = 2, b_3 = 2, b_4 = 3\}, \tag{3.32}$$

$$\overline{\text{PS}}_w = \frac{\left(1 - \frac{x_4}{2}\right)}{2N_1(x_3, \frac{x_4}{2}, \lambda)}, \quad \overline{\text{PS}} = \frac{\left(1 - \frac{x_3 x_4}{2}\right)\left(1 - \frac{x_4}{2}\right)^2}{2N_1^2(x_3, \frac{x_4}{2}, \lambda)},$$

$$\underline{\text{sector } 4}: \quad \{a_1 = 4, a_2 = 3, a_3 = 2, a_4 = 1\}, \quad \{b_1 = 4, b_2 = 3, b_3 = 2, b_4 = 1\},$$

$$\overline{\text{PS}}_w = \frac{\left(1 - \frac{x_2 x_4}{2}\right)}{2N_1(x_3, \frac{x_4 x_2}{2}, \lambda)}, \quad \overline{\text{PS}} = \frac{\left(1 - \frac{x_2 x_3 x_4}{2}\right)\left(1 - \frac{x_2 x_4}{2}\right)^2}{2N_1^2(x_3, \frac{x_4 x_2}{2}, \lambda)},$$

$$\underline{\text{sector } 5}: \quad \{a_1 = 4, a_2 = 2, a_3 = 2, a_4 = 2\}, \quad \{b_1 = 4, b_2 = 2, b_3 = 2, b_4 = 2\},$$

$$\overline{\text{PS}}_w = \frac{1}{4N_1(x_3, 1 - \frac{x_4}{2}, \lambda)}, \quad \overline{\text{PS}} = \frac{(1 - \frac{x_4}{2})(1 - x_3(1 - \frac{x_4}{2}))}{4N_1^2(x_3, 1 - \frac{x_4}{2}, \lambda)}.$$

The function N_1 is given by

$$N_1(x_3, x_4, \lambda) = 1 + x_4(1 - 2x_3) - 2(1 - 2\lambda)\sqrt{x_4(1 - x_3)(1 - x_3 x_4)}. \tag{3.33}$$

It is straightforward to use momentum and phase-space parametrizations described above to extract singularities from matrix elements squared in a factorized form, thereby facilitating the integration over the full phase-space with the help of plus-distribution expansions. We will briefly discuss this in the next Section.

We note that the phase-space parametrization that we just described resolves all the singularities of the matrix elements for the final state with a b-quark and two gluons. The process with a b-quark and two additional massless quarks in the final state has a simpler singularity structure than the two-gluon case, so our phase-space parametrization should be applicable to the quark case as well. However, the quark case is different in that quark amplitudes are, in general, not symmetric with respect to q and $\bar{q}$ permutation and also they are less singular. It is therefore useful to consider $bq\bar{q}$ final state separately and design a parametrization of the phase-space for this case. We start by listing kinematic configurations that lead to non-integrable singularities in the amplitude $t \to b + q(p_3) + \bar{q}(p_4) + e^+ + \nu$. From the point of view of the singularity structure it is sufficient to understand the singlet contribution where the flavor of the $q\bar{q}$-pair is different from b. The case of $bb\bar{b}$ final state then easily follows. The singular configurations that we need to consider are $i)$ both q and $\bar{q}$ are soft; $ii)$ both q and $\bar{q}$ are collinear to the $b-$quark and $iii)$ q and $\bar{q}$ are collinear to each other. Analyzing these singular limits, we conclude that the number of sectors that we need to consider for $bq\bar{q}$ final state is four. Momenta are parametrized as in the gluon case. The first two sectors are

- sector 1: $E_3 = x_1 E_{\max}$, $\quad E_4 = x_1 x_2 x_{\max} E_{\max}$, $\quad \eta_3 = x_3$, $\quad \eta_4 = x_3(1 - x_4)$,

- sector 2: $E_3 = x_1 E_{\max}$, $\quad E_4 = x_1 x_2 x_{\max} E_{\max}$, $\quad \eta_3 = x_3(1 - x_4)$, $\quad \eta_4 = x_3$,

---

[3]We suppress the sector label everywhere in the equations below.

and the other two are obtained from sectors 1 and 2 by permuting p_3 and p_4. Finally, all quark sectors share the same phase-space. It reads

$$
\begin{aligned}
d\Pi_{bq\bar{q}e^+\nu} = \Upsilon(\epsilon) & \left[\frac{\Gamma(1+\epsilon)}{(4\pi)^{-\epsilon}} \frac{1}{8\pi^2} \right]^2 N_{\mathrm{BW}} \left(\frac{\Gamma(1-\epsilon)}{\Gamma(1+\epsilon)\Gamma(1-2\epsilon)} \right)^2 \\
& \times \frac{1}{8\pi^2} \frac{E_b E_{\max}^4 x_{\max}^2}{(Q_0 - Q_3)} \frac{x_2}{N_1(x_3, 1-x_4, \lambda)} \mathrm{PS}^{-\epsilon} \\
& \times \frac{dx_1}{x_1^{1+4\epsilon}} \frac{dx_3}{x_3^{1+2\epsilon}} \frac{dx_4}{x_4^{1+2\epsilon}} dx_2 dx_5 dx_6 dx_7 dx_8 dx_9 [x_1^4 x_3^2 x_4^2],
\end{aligned}
\tag{3.34}
$$

where

$$
\mathrm{PS} = \frac{1024 E_b^2 E_{\max}^2 x_2^2 x_{\max}^2}{N_1^2(x_3, 1-x_4, \lambda)} \lambda (1-\lambda)(1-x_3)(1-x_4)(1-x_3(1-x_4)) \sin^2 \varphi_3.
\tag{3.35}
$$

It follows from the phase-space parametrization that we do not intend to construct the plus-distribution expansion with respect to the variable x_2. This is done intentionally since $x_2 \to 0$ corresponds to a single-soft limit which is not singular for the $q\bar{q}b$ final state.

4 Singular limits

The phase-space parametrization that we discussed in the previous Section is optimized for extracting the singular behavior of scattering amplitudes. This is done by exploiting universal soft and collinear limits of these amplitudes. The goal of this Section is to describe the limits that we require for the top quark decay. We begin with the discussion of the relevant soft limits and then consider the collinear ones.

Soft singularities can only occur if gluons become soft.[4] In general, emissions of soft particles lead to color correlations but because in the top quark decay the number of colored particles is small, all color correlations simplify and the relevant soft limits can be written in a compact form. For example, the single soft limit of the $t \to b + g(p_3) + e^+ + \nu$ amplitude squared reads

$$
|\mathcal{M}(t, b, g)|^2 \approx g_s^2 C_F |\mathcal{M}(t, b)|^2 S_{tb}(p_3),
\tag{4.1}
$$

where the eikonal factor S_{tb} is

$$
S_{tb}(p_3) = \frac{2p_t \cdot p_b}{(p_t \cdot p_3)(p_b \cdot p_3)} - \frac{m_t^2}{(p_t \cdot p_3)^2}.
\tag{4.2}
$$

Note that for a single-gluon emission process $t \to b + g(p_3) + e^+ + \nu$ the function $F(x_1, x_2)$ is given by

$$
F(x_1, x_2) = x_1^2 x_2 |\mathcal{M}(t, b, g)|^2,
\tag{4.3}
$$

where x_1 and x_2 parametrize the gluon energy $E_3 = E_{\max} x_1$ and the relative angle with respect to the b-momentum, $p_b \cdot p_3 = 2E_b E_3 x_2$. We have seen that we need $F(x_1 = 0, x_2)$ for the computation and we now show how to obtain it from the soft limit Eq.(4.1). The key point is that the dependence on the gluon momentum in the right hand side of Eq.(4.1) is entirely contained in the eikonal factor. Hence, to find $F(x_1 = 0, x_2)$, we need

$$
\lim_{x_1 \to 0} x_1^2 x_2 S_{tb}(p_3) = E_{\max}^{-2}(1-x_2).
\tag{4.4}
$$

---

[4]In the process $t \to b + q + \bar{q} + e^+ + \nu$ there is also a soft singularity when energies of *both* q and $\bar{q}$ vanish. We do not discuss this case as it follows from the soft limit of $t \to b + g + e^+ + \nu$.

While the single soft limit provides a very simple example, we note that the same approach is used to compute limiting values of integrand functions F also for more complex cases, such as limits of double-real emission amplitudes squared and limits of one-loop contributions to single-real emission processes. We will not discuss these derivations; instead, we limit ourselves to the presentation of the relevant ingredients in what follows.

The double soft limit of the amplitude squared for $t \to b + g(p_3) + g(p_4) + e^+ + \nu$ is only slightly more complicated than the single soft limit. We can write it as

$$
\begin{aligned}
|\mathcal{M}(t,b,g_3,g_4)|^2 \approx & g_s^4 |\mathcal{M}(t,b)|^2 C_F \left(C_A (2S_{tb}(p_3,p_4) - S_{tt}(p_3,p_4) - S_{bb}(p_3,p_4)) \right. \\
& \left. + C_F S_{tb}(p_3) S_{tb}(p_4) \right).
\end{aligned}
\tag{4.5}
$$

The double-emission eikonal factors depend on the masses of the emitters; they can be extracted from Refs.[30, 55]. For completeness, we present them below for the specific cases that we need to describe top quark decays. In the massless case $p_b^2 = 0$, we find

$$
S_{bb}(p_3,p_4) = 2(1-\epsilon) \frac{(p_b \cdot p_3)(p_b \cdot p_4)}{(p_3 \cdot p_4)^2 (p_b \cdot p_{34})^2},
\tag{4.6}
$$

where $p_{34} = p_3 + p_4$. In the massive case $p_t^2 = m_t^2$, the double eikonal factor reads

$$
\begin{aligned}
S_{tt}(p_3,p_4) = & 2(1-\epsilon) \frac{(p_t \cdot p_3)(p_t \cdot p_4)}{(p_3 \cdot p_4)^2 (p_t \cdot p_{34})^2} + \frac{m_t^4}{(p_t \cdot p_3)(p_t \cdot p_4)(p_t \cdot p_{34})^2} + \\
& + \frac{3}{2} \frac{m_t^2}{(p_3 \cdot p_4)(p_t \cdot p_3)(p_t \cdot p_4)} - \frac{m_t^2}{(p_3 \cdot p_4)(p_t \cdot p_{34})^2} \left(\frac{p_t \cdot p_3}{p_t \cdot p_4} + \frac{p_t \cdot p_4}{p_t \cdot p_3} + 4 \right).
\end{aligned}
\tag{4.7}
$$

Finally, we give an expression for the eikonal factor $S_{tb}(p_3,p_4)$, where $p_t^2 = m_t^2$ and $p_b^2 = 0$. It reads

$$
\begin{aligned}
S_{tb}(p_3,p_4) = & (1-\epsilon) \frac{(p_b \cdot p_4)(p_t \cdot p_3) + (p_b \cdot p_3)(p_t \cdot p_4)}{(p_3 \cdot p_4)^2 (p_b \cdot p_{34})(p_t \cdot p_{34})} + \frac{p_b \cdot p_t}{p_3 \cdot p_4} \left(\frac{1}{(p_b \cdot p_3)(p_t \cdot p_4)} + \right. \\
& + \frac{1}{(p_b \cdot p_4)(p_t \cdot p_3)} - \frac{1}{(p_b \cdot p_{34})(p_t \cdot p_{34})} \left(3 + \frac{(p_b \cdot p_4)(p_t \cdot p_3)}{2(p_b \cdot p_3)(p_t \cdot p_4)} + \frac{(p_b \cdot p_3)(p_t \cdot p_4)}{2(p_b \cdot p_4)(p_t \cdot p_3)} \right) \bigg) + \\
& - \frac{(p_b \cdot p_t)^2}{(p_b \cdot p_3)(p_b \cdot p_4)(p_t \cdot p_3)(p_t \cdot p_4)} \left(1 - \frac{(p_b \cdot p_3)(p_t \cdot p_4) + (p_b \cdot p_4)(p_t \cdot p_3)}{2(p_b \cdot p_{34})(p_t \cdot p_{34})} \right) + \\
& + m_t^2 \left(\frac{(p_b \cdot p_t)}{2(p_b \cdot p_3)(p_b \cdot p_4)(p_t \cdot p_3)(p_t \cdot p_4)} \frac{p_b \cdot p_{34}}{p_t \cdot p_{34}} - \frac{1}{4(p_3 \cdot p_4)(p_t \cdot p_3)(p_t \cdot p_4)} + \right. \\
& \left. - \frac{1}{2(p_3 \cdot p_4)(p_b \cdot p_{34})(p_t \cdot p_{34})} \left(\frac{(p_b \cdot p_3)^2}{(p_b \cdot p_4)(p_t \cdot p_3)} + \frac{(p_b \cdot p_4)^2}{(p_b \cdot p_3)(p_t \cdot p_4)} \right) \right).
\end{aligned}
\tag{4.8}
$$

It is straightforward to check, using momenta parametrization in terms of x-variables for various types of sectors for double-real emission described in Section 3, that all overlapping singularities get resolved in the sum of the eikonal factors Eq.(4.5) and that the subtraction terms for the soft limits of the double-real emission process can be calculated.

In order to subtract soft singularities from one-loop amplitudes for $t \to b + g(p_3) + e^+ + \nu$, we need the expression for the eikonal current to one-loop. The massless result for the one-loop soft current was obtained in Ref. [56]. The one-loop massive soft current was computed in Ref. [57]. We have re-calculated this soft current for the top quark decay into a bottom quark and present the result of the calculation below. This result is identical to Ref. [57] but it is written in the kinematic region

which is relevant for the top quark decay, so that no analytic continuation is required. The soft limit of the interference of one-loop and tree-level amplitudes is written in Eq.(2.10). The one-loop eikonal factor reads

$$S_{tb}^{(1)}(p_3) = g_s^2 C_F S_{tb}(p_3) 2\text{Re}\left[\mathcal{I}_{tb}(p_t, p_b, p_3)\right],\tag{4.9}$$

where

$$
\begin{aligned}
\mathcal{I}_{tb} = &-\frac{(p_t \cdot p_b)}{m_t^2(p_b \cdot p_3)^2 - 2(p_t \cdot p_b)(p_t \cdot p_3)(p_b \cdot p_3)}\left\{2(p_t \cdot p_3)^2(p_b \cdot p_3)I_1\right.\\
&+ 2(p_t \cdot p_3)(p_t \cdot p_b)(p_b \cdot p_3)I_2 + 2(p_b \cdot p_3)\left[(p_t \cdot p_b)(p_t \cdot p_3) - m_t^2(p_b \cdot p_3)\right]I_3\\
&+ 4\left[(p_t \cdot p_b)(p_t \cdot p_3)(p_b \cdot p_3) - m_t^2(p_b \cdot p_3)^2\right]\frac{(p_t \cdot p_3)(p_b \cdot p_3)}{(p_t \cdot p_b)}I_4\left.\right\}.
\end{aligned}
\tag{4.10}
$$

The Feynman integrals $I_{1,..4}$ in Eq.(4.10) are defined as

$$
\begin{aligned}
I_1 &= \int \frac{d^d k}{i(2\pi)^d}\frac{1}{(k+p_3)^2 k^2(2p_t \cdot k)}, & I_2 &= \int \frac{d^d k}{i(2\pi)^d}\frac{1}{k^2(2p_t \cdot k)(2p_b \cdot k + 2p_b \cdot p_3)},\\
I_3 &= \int \frac{d^d k}{i(2\pi)^d}\frac{1}{k^2(2p_b \cdot k)(2p_t \cdot k - 2p_t \cdot p_3)}, & I_4 &= \int \frac{d^d k}{i(2\pi)^d}\frac{1}{(k-p_3)^2 k^2(2p_b \cdot k)(2p_t \cdot k - 2p_t \cdot p_3)}.
\end{aligned}
\tag{4.11}
$$

We note that each propagator implicitly includes $+i0$-prescription that unambiguously specifies the relevant analytic continuation of the result. The integrals are computed to be (see Appendix B for details)

$$
\begin{aligned}
I_1 &= \frac{\Gamma(-\epsilon)\Gamma(2\epsilon)m_t^{2\epsilon}}{(4\pi)^{d/2}(s_{t3})^{1+2\epsilon}}, & I_2 &= -\frac{\Gamma(1-2\epsilon)\Gamma(\epsilon)\Gamma(2\epsilon)m_t^{-2\epsilon}e^{2\pi i\epsilon}}{(4\pi)^{d/2}(s_{b3})^{2\epsilon}(s_{tb})^{1-2\epsilon}}, & I_3 &= -\frac{\Gamma(-\epsilon)\Gamma(2\epsilon)m_t^{2\epsilon}}{(4\pi)^{d/2}(s_{t3})^{2\epsilon}s_{tb}},\\
I_4 &= -\frac{\Gamma(-\epsilon)\Gamma(1+2\epsilon)m_t^{2\epsilon}}{(4\pi)^{d/2}(x_2)^\epsilon(s_{t3})^{1+2\epsilon}s_{b3}}\left[e^{2\pi i\epsilon}\frac{\Gamma(1+\epsilon)\Gamma(-2\epsilon)}{\Gamma(1-\epsilon)}F_{21}(-\epsilon,1+\epsilon,1-\epsilon;1-x_2)\right.\\
&\qquad\left.-\frac{1}{\epsilon}F_{21}(-\epsilon,-\epsilon,1-\epsilon;1-x_2)\right],
\end{aligned}
\tag{4.12}
$$

where $s_{ij} = 2p_i \cdot p_j$ and $x_2 = (m_t^2 s_{b3})/(s_{tb}s_{t3})$. We emphasize that products of all four-momenta are positive-definite since we write the results for the soft current in the correct kinematic region. We note that to use the results Eq.(4.12) in our plus-distribution expansion, we should extract all the relevant branch-cuts from the hypergeometric functions.

We now turn to the discussion of collinear singularities. It is well-known that in the collinear limit any matrix element squared factorizes into a splitting function that is, in general, spin-dependent, and a reduced squared matrix element that depends only on the sum of momenta of collinear particles. For the top quark decay, we need to describe such collinear splitting processes as $b \to b+g$, $b \to b+g+g$, $g \to g+g$, $b \to b+q+\bar{q}$, $b \to b+b\bar{b}$ and $g \to q\bar{q}$. The corresponding splitting functions can be found in Ref. [55]. Many splitting functions that we need for top quark decay do not contain spin-correlations. The corresponding factorization formula reads

$$|\mathcal{M}|^2 \sim s_c^{-1}\, P(\{z\})|\tilde{\mathcal{M}}|^2,\tag{4.13}$$

where $\tilde{\mathcal{M}}$ is the reduced amplitude, s_c is the scalar product of collinear momenta that vanishes in the exact collinear limit and $P(\{z\})$ is a splitting function that depends on the set of energy fractions $\{z\}$. This is an easy case to deal with since, in this situation, the collinear limit depends on the reduced

amplitude squared which can be computed in the standard way. However, there are two splitting functions that we have to deal with ($g \to gg$, $g \to q\bar{q}$), that do contain spin correlations. In that case, the collinear limit is more complicated

$$|\mathcal{M}|^2 \sim s_c^{-1} \, P^{\mu\nu}(\{z\}) \tilde{\mathcal{M}}^\mu \tilde{\mathcal{M}}^{\nu,*}. \tag{4.14}$$

Any spin-dependent splitting function $P^{\mu\nu}(z)$ can be written as

$$P(z) = -g^{\mu\nu} P_1(z, \epsilon) + n^\mu n^\nu P_2(z, \epsilon), \tag{4.15}$$

where n^μ is a four-vector that specifies how the collinear direction is approached. To compute the right hand side in Eq.(4.14), it is useful to re-write it through helicity amplitudes. This is easy to do since gauge-invariance of scattering amplitudes allows us to replace $g^{\mu\nu}$ and $n^\mu n^\nu$ in Eq.(4.15) by rank-two tensors constructed from polarization vectors

$$-g_{\mu\nu} = \sum_{\lambda=\pm} \epsilon_\mu(\lambda)\epsilon_\nu^*(\lambda), \quad n^\mu n^\nu = \sum_{\lambda_1=\pm,\lambda_2=\pm} [n \cdot \epsilon(\lambda_1) \, n \cdot \epsilon(\lambda_2)] \, \epsilon_\mu^*(\lambda_1)\epsilon_\nu^*(\lambda_2). \tag{4.16}$$

We note that, since we work in dimensional regularization, it is important to extend the sum over four-dimensional gluon helicities in Eq.(4.16), to include ϵ-dimensional polarization vectors as well. It is possible to do so by introducing "scalar" polarizations of gluons that point along Cartesian components of the ϵ-dimensional sub-space of the full d-dimensional Minkowski space. In Section 5 we will return to the issue of spin-correlations, to discuss a consistent implementation of angular variables in our phase-space parametrization.

While the majority of collinear limits is completely determined by the known splitting functions [55], there are a few cases when further computations are required. This happens for example in the strongly-ordered limit of the $b \to g(p_3)g(p_4)b$ splitting function. The strongly-ordered limit occurs when the two gluons are much more collinear to each other than to the b-quark, i.e. $p_3 \cdot p_4 \ll p_b \cdot p_3 + p_b \cdot p_4$. In this case the full matrix element factorizes as

$$|\mathcal{M}(t, b, g_3, g_4)|^2 \approx \frac{g_s^2}{(2p_3 \cdot p_4)(2p_b \cdot p_3 + 2p_b \cdot p_4)} \hat{P}_{g_3 g_4 b}^{\text{s.o.}} |\mathcal{M}(t, b)|^2. \tag{4.17}$$

We derive the following result for the strongly-ordered limit of the $b \to g(p_3)g(p_4)b$ splitting function

$$\begin{aligned}
\hat{P}_{g_3 g_4 b}^{\text{s.o.}} = {} & 8 C_F C_A \left[\frac{4\lambda z_3(1-z_3)z_b}{1-z_b} + \frac{1 + (z_3(1-z_3)(1-z_b))^2 + z_b^2 - 2z_3(1-z_3)(1+z_b^2)}{(1-z_b)z_3(1-z_3)} \right] \\
& + 8 C_F C_A \left[(1-z_b)\left(2 - z_3(1-z_3) - \frac{1}{z_3(1-z_3)} \right) - \frac{4\lambda z_3(1-z_3)z_b}{1-z_b} \right] \epsilon + \mathcal{O}(\epsilon^3),
\end{aligned} \tag{4.18}$$

where $z_3 = E_3/(E_3 + E_4)$, $z_b = E_b/(E_3 + E_4 + E_b)$ and λ is one of the phase-space variables introduced in Section 3.

5 How to treat spin-correlations consistently in the NNLO computation

As we pointed out earlier, it is plausible, but not entirely obvious, that one can consistently treat positron and neutrino momenta as four-dimensional in higher-order perturbative computations. The goal of this Section is to elaborate on this point. We will discuss it in a slightly simplified setting, by considering top quark decay into a polarized W-boson, ignoring W-decays into leptons.

We want to treat the polarization vector of the W-boson as a four-dimensional vector. In addition, there are other vectors that we would like to treat as four-dimensional; they include the W-momentum, the top quark momentum and the b-quark momentum. Assuming that we are in the top quark rest frame and making use of momentum conservation, we conclude that we can embed the momentum of one additional gluon to the four-dimensional space, but that the second gluon must have additional ϵ-dimensional components. This means that the phase-space parametrization for single-gluon emission processes that we discussed in Section 3 is perfectly valid but the phase-space parametrization for double-real emission computations must be extended. To this end, we parametrize momenta and the W-polarization vector as

$$p_t = (m_t, \vec{0}; 0), \ p_b = E_b(1, \vec{0}, 1; 0), \ p_W = (E_W, p_w^x, 0, p_W^y; 0), \ \epsilon_W = (\epsilon_W^{(0)}, \epsilon_W^{(x)}, \epsilon_W^{(y)}, \epsilon_W^{(z)}; 0),$$
$$p_{g_3} = E_{g_3}(1, \sin\theta_3 \cos\varphi_3, \sin\theta_3 \sin\varphi_3 \cos\alpha, \cos\theta_3; \sin\theta_3 \sin\varphi_3 \sin\alpha),$$
(5.1)

and determine p_{g_4} using momentum conservation. A component of a four-vector in Eq.(5.1) shown after the semi-column is the ϵ-dimensional component. We now perform a rotation in the $y - \epsilon$ plane, to remove the ϵ-dimensional part of the gluon momentum p_{g_3}. From momentum parametrization of other particles it follows that this rotation does not induce ϵ-dimensional components for any of them. On the other hand, such ϵ-components appear in the polarization vector ϵ_W of the W-boson after the rotation.

To understand in which cases we require the ϵ-dimensional components in W-polarization, we consider singular limits. These limits can be divided into two groups. Some limits lead to expressions where squares of reduced matrix elements appear. The reduced matrix elements squared can be either leading order or next-to-leading order. In both cases, because of the choice of the momenta above, we conclude that

$$|\mathcal{M}|^2_{\mathrm{LO,NLO}}(p_t, p_b, p_W, \epsilon_W(\alpha)) = |\mathcal{M}|^2_{\mathrm{LO,NLO}}(p_t, p_b, p_W, \epsilon_W(0)),$$
(5.2)

where α parametrizes the ϵ-dimensional angle and $\alpha = 0$ corresponds to the four-dimensional limit, see Eq.(5.1). We note that Eq.(5.2) is valid because through next-to-leading order none of the vectors contains y-components that can lead to an α-dependence through products with $\epsilon_W(\alpha)$. Therefore, in all limits that are proportional to the reduced matrix elements squared, we can neglect the dependence of the W-polarization vector on the extra-dimensional angle α, provided that the normalization condition $\epsilon_W^2 = -1$ is maintained.

A different situation occurs when spin correlations appear in the singular limits. In the top quark decay case, there are no triple-collinear limits which have this feature and we only need to focus on double-collinear limits. As an example, we take the case when gluon g_3 and gluon g_4 are collinear. The collinear limit is written as

$$|\mathcal{M}_{t \to bWg_3g_4}|^2 \sim P_{\mu\nu}\mathcal{M}^\mu \mathcal{M}^\nu = (-g_{\mu\nu}P_1(z, \epsilon) + P_2(z, \epsilon)n^\mu n^\nu)\mathcal{M}^\mu_{t \to bWg_{34}}\mathcal{M}^\nu_{t \to bWg_{34}},$$
(5.3)

and n^μ is the vector that describes how vectors p_{g_3,g_4} approach the collinear direction. The matrix element $\mathcal{M}^\mu_{t \to bWg_{34}}$ contains the polarization of the W-boson and depends on momenta of t, b and W. Since none of these momenta have y-components, we can remove the α-dependence from the matrix element by rotating all vectors in the $y - \epsilon$ plane. Since, in general, the vector n^μ *does have* a y-component, such a rotation induces an α-dependence in the splitting function. The vector n^μ becomes

$$n^\mu \to \pm\sqrt{\lambda}\bar{n}^\mu + \sqrt{1-\lambda}\left(\cos\alpha \tilde{n}^\mu + \sin\alpha n_5^\mu\right),$$
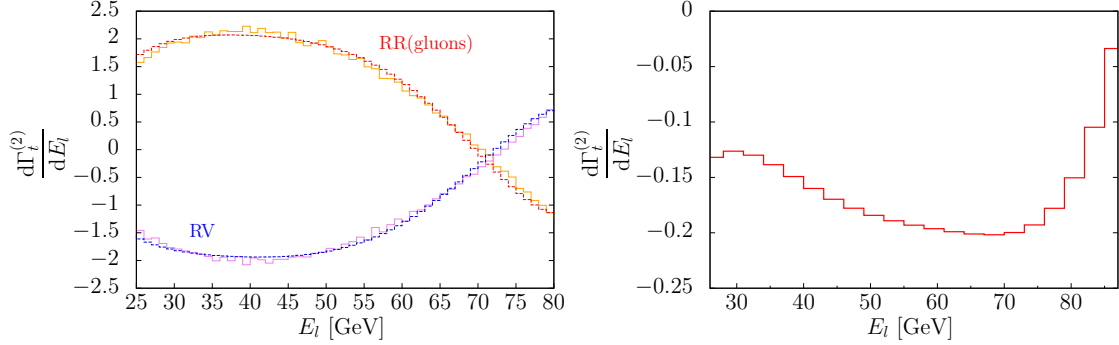(5.4)

Figure 1. Distribution of the second order coefficient $d\Gamma_t^{(2)}$ in the positron energy. Left pane: double-real and real-virtual contributions. Original histograms are shown with solid lines; Legendre polynomial fit is shown with dashed lines. Right pane: distribution of $d\Gamma_t^{(2)}$ in the lepton energy. See text for details.

where $\bar{n}^\mu = [\cos\theta_3 \cos\varphi_3, \cos\theta_3 \sin\varphi_3, -\sin\theta_3; 0]$, $\tilde{n}^\mu = [-\sin\varphi_3, \cos\varphi_3, 0; 0]$ and $n_5^\mu = [0, 0, 0; 1]$. The two possible signs in front of the first vector are for different sectors. Since we do not need the α-angle for any other limit, it should decouple from the point-by-point subtraction. This allows us to average over α and modify the spin-correlated part of the splitting function by including "integrated" terms. Using the two non-vanishing averages

$$\langle \cos^2 \alpha \rangle = \frac{1}{1 - 2\epsilon}, \quad \langle \sin^2 \alpha \rangle = \frac{-2\epsilon}{1 - 2\epsilon}, \tag{5.5}$$

we find the replacement rule

$$n^\mu n^\nu \to \lambda \bar{n}^\mu \bar{n}^\nu + \frac{2\epsilon(1 - \lambda)}{1 - 2\epsilon} \left(\tilde{n}^\mu \tilde{n}^\nu - n_5^\mu n_5^\nu \right). \tag{5.6}$$

Applying it to Eq.(5.3) and treating all the vectors in the matrix element $\mathcal{M}$, including W-polarization, as four-dimensional, we get an easy way to consistently combine dimensional regularization with four-dimensional handling of all the relevant vectors that we have in the process. Finally, we note that it is obvious how to generalize this discussion to account for the W-boson decays to a lepton pair.

6 Results

In this Section we show some results of our computation. We note that our goal in this paper is not to provide extensive phenomenological studies of top quark decays but to illustrate the capabilities of the computational method. The results that we present below are selected accordingly.

We remind the reader that we consider the top quark decay into hadronic final states and a single lepton pair $t \to b + X_{\text{hadr}} + e^+ + \nu$. We use the on-shell renormalization scheme for the top quark and the $\overline{\text{MS}}$ renormalization scheme for the strong coupling constant in a theory with five massless flavors. We set the renormalization scale to the value of the top quark mass $\mu = m_t$. Results for $\mu \neq m_t$ can be immediately obtained by using renormalization group equations, so we do not present them here. In our computation, we account exactly for the off-shellness of the W-boson. The reasons for doing that are explained in the Introduction.

To show the quality of our numerical computation, we isolate all the different color structures that contribute to the final result

$$\Gamma_t = \Gamma_t^{(0)} \left[1 + C_F \frac{\alpha_s}{2\pi} \Delta_1 + \left(\frac{\alpha_s}{2\pi} \right)^2 \left(C_F^2 \Delta_A + C_F C_A \Delta_{NA} + C_F T_R n_l \Delta_l + C_F T_R \Delta_h \right) \right] + \mathcal{O}(\alpha_s^3). \tag{6.1}$$

The different contributions to second order corrections were computed in a number of papers a decade ago for top quark decays to an on-shell W boson. Since $\Delta_{A,NA,l,h}$, as defined in Eq.(6.1), are *relative* corrections, we expect that the importance of the W-off-shellness effect is reduced. We use the analytic computation of Refs. [20, 21] performed as an expansion in m_W/m_t, to infer numerical values for the coefficients. We employ the input parameters $m_t = 172.85$ GeV and $m_W = 80.419$ GeV to obtain [20, 21]

$$C_F T_R \Delta_l = 7.978, \quad C_F T_R \Delta_h = -0.1166, \quad C_F^2 \Delta_A = 23.939, \quad C_F C_A \Delta_{NA} = -134.24. \qquad (6.2)$$

We compare these results of the analytic computation [20, 21] with our *numerical* results. We find[5]

$$\begin{aligned} C_F T_R \Delta_l^{\text{num}} &= 7.970(6), \quad C_F T_R \Delta_h^{\text{num}} = -0.11662(1), \\ C_F^2 \Delta_A^{\text{num}} &= 24.38(25), \quad\ \ C_F C_A \Delta_{NA}^{\text{num}} = -133.6(4), \end{aligned} \qquad (6.3)$$

where integration errors are explicitly shown. By comparing Eq.(6.2) and Eq.(6.3), we find good agreement between results of analytic and numerical computations. The level of agreement is rather striking since there are large cancellations between various contributions to the NNLO final result. To illustrate this point, we show individual contributions to the abelian coefficient $C_F^2 \Delta_A^{\text{num}}$ with their integration errors. They read

$$\begin{aligned} C_F^2 \Delta_{A,\text{RR}} &= -127.12(23), \qquad C_F^2 \Delta_{A,\text{RV}} = 60.24(6), \quad C_F^2 \Delta_{A,\text{VV}} = 83.0154(5), \\ C_F^2 \Delta_{A,\text{ren}} &= 16.513(12), \qquad C_F^2 \Delta_{A,q\bar{q}} = -8.227(2), \\ C_F^2 \Delta_A &= C_F^2 \Delta_{A,\text{RR}} + C_F^2 \Delta_{A,\text{RV}} + C_F^2 \Delta_{A,\text{VV}} + C_F^2 \Delta_{A,\text{ren}} + C_F^2 \Delta_{A,q\bar{q}} = 24.38(25), \end{aligned}$$

where we include double-real (RR), real-virtual (RV), two-loop virtual (VV), renormalization and quark-pair corrections. Comparing individual contributions with the final result for Δ_A, we observe very significant cancellations. It is therefore quite remarkable that we can maintain $\mathcal{O}(1\%)$ error on the NNLO coefficient.

We now turn to the discussion of kinematic distributions. To facilitate this discussion, we write the differential decay rate as

$$d\Gamma_t = d\Gamma_t^{(0)} + \left(\frac{\alpha_s}{2\pi}\right) d\Gamma_t^{(1)} + \left(\frac{\alpha_s}{2\pi}\right)^2 d\Gamma_t^{(2)} + \mathcal{O}(\alpha_s^3), \qquad (6.4)$$

and plot $d\Gamma_t^{(2)}/dx$ in Figs. 1, 2 for various observables x. In particular, in Fig. 1 we show $d\Gamma_t^{(2)}/dE_l$, where E_l is the positron energy. The final result for NNLO QCD corrections arises as a result of large cancellations between various contributions, most notably the double-real and the real-virtual ones. To illustrate this point, we show these contributions individually in the left pane and the sum of all contributions to $d\Gamma_t^{(2)}/dE_l$ in the right pane. We note that at smaller values of E_l the final result is about ten times smaller than double-real and real-virtual contributions separately. At this level of cancellations, bin-bin fluctuations that are barely seen for double-real and real-virtual contributions individually (left pane in Fig. 1) become a serious issue. To overcome it, we choose to fit individual contributions to the sum of Legendre polynomials and then add fitted results rather than original histograms. Upon doing that, we find that our final result for $d\Gamma_t^{(2)}/dE_l$ exhibits a re-assuring pattern. Suppose, we account for N_L Legendre polynomials in the fit. If N_L is too small, we find that the resulting $d\Gamma_t^{(2)}/dE_l$ is not stable against including more polynomials into the fit. If N_L is too

---

[5] All numerical results presented in this Section are obtained using the adaptive Monte-Carlo algorithm VEGAS [58] as implemented in the CUBA library [59].
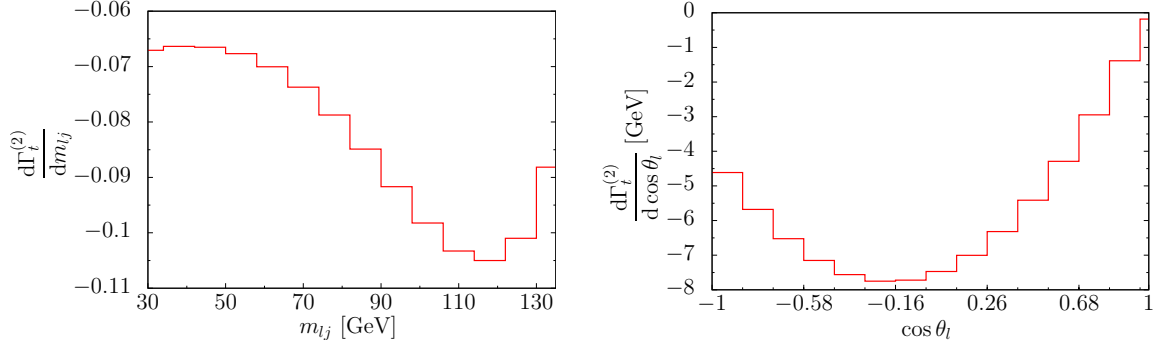
Figure 2. Left pane: distribution of the second order coefficient $\mathrm{d}\Gamma_t^{(2)}$ in invariant mass of the positron and the hardest jet. Right pane: distribution of the second order coefficient $\mathrm{d}\Gamma_t^{(2)}$ in the opening angle of the positron with respect to the W-direction of motion, in the W-rest frame. See text for details.

large, we fit bin-bin fluctuations and do not gain anything. However, we find that there is a range of intermediate values of N_L that we can use in the fit so that, on one hand, our final result for $\mathrm{d}\Gamma_t^{(2)}/\mathrm{d}E_l$ does no depend on the exact value of N_L and, on the other hand, the resulting distribution is smooth. Distributions shown in the right pane of Fig. 1 and in Fig. 2 are obtained following this procedure.

In the left pane of Fig. 2 we show NNLO QCD contributions to the kinematic distribution in the invariant mass of the positron and the hardest (in energy) jet in the event. The jet here is defined with the lepton collider $k_\perp$-algorithm where the distance between two partons i and j is given by $y_{ij} = 2\min(E_i^2/m_t^2, E_j^2/m_t^2)(1 - \cos\theta_{ij})$. The relative angle θ_{ij} is defined in the top quark rest frame. For numerical computations, we take $y_{ij} = 0.1$. In the right pane of Fig. 2 we show NNLO QCD correction to the kinematic distribution of the positron polar angle defined in the W-boson rest frame, relative to the direction of motion of the W-boson[6]. This distribution is interesting because it allows us to determine helicity fractions of the W-bosons in top decays. Indeed, to all orders in QCD perturbation theory, the decay rate can be written as

$$\frac{\mathrm{d}\Gamma_t}{\mathrm{d}\cos\theta_l} = \frac{3}{4}\sin^2\theta_l\,\Gamma_L + \frac{3}{8}\left(1 + \cos\theta_l\right)^2\Gamma_+ + \frac{3}{8}\left(1 - \cos\theta_l\right)^2\Gamma_-. \tag{6.5}$$

The widths $\Gamma_L, \Gamma_\pm$ define partial decay rates into polarized W-bosons. The helicity fractions are constructed from partial widths as $F_{\pm,L} = \Gamma_{\pm,L}/\Gamma_t$, where $\Gamma_t = \Gamma_+ + \Gamma_- + \Gamma_L$. Our result for $\mathrm{d}\Gamma_t/\mathrm{d}\cos\theta_l$ shown in Fig. 2 allows us to compute the NNLO QCD corrections to the helicity fractions. Upon doing so, we find good agreement with similar results presented in Ref. [22]. For example, by fitting the angular distribution shown in the right pane of Fig. 2 we find the NNLO QCD contributions to helicity fractions[7] $[\delta F_L, \delta F_-, \delta F_+] = [-0.0022(1), 0.0021(1), 0.0001(1)]$. These numbers should be compared to the results of analytic computations reported in Ref. [22], $[\delta F_L, \delta F_-, \delta F_+] = [-0.0023, 0.0021, 0.0002]$. A good agreement between the two results is obvious.

7 Conclusions

In this paper we described a computation of NNLO QCD corrections to semileptonic decays of the top quark at a fully-differential level. We have used a framework described in Refs. [29, 30, 35] that

---

[6]The momentum of the W-boson can be determined from the momentum of the recoiling hadronic system in top decay.

[7]The exact definition of the helicity fractions and values of α_s used to obtain these results can be found in Ref. [22].

combines sector-decomposition and Frixione-Kunszt-Signer phase-space partitioning to disentangle overlapping kinematic regions that may lead to soft and collinear singularities. We have shown that this technique works in the same way as parton level Monte Carlo integrators at next-to-leading order, so that weighted events can be generated and a variety of kinematic distributions can be computed in a single run of the program.

There is a number of phenomenological applications of the calculation reported in this paper that we envision. Eventually, it will be combined with the perturbative QCD description of the top quark production process, to provide NNLO QCD results for $pp \to t\bar{t} \to W^+W^-b\bar{b}$ in the narrow width approximation. It can also be used to investigate the dependence of various observables studied in top quark decays, for example the helicity fractions, on kinematic cuts applied to top quark decay products. A minor modification of our calculation turns it into a NNLO QCD result for the most important contribution to the single top production process in hadron collisions. Finally, as explained in the Introduction, our calculation can be adapted to explore the impact of NNLO QCD corrections to inclusive charmless semileptonic decays of b-quarks on the determination of the CKM matrix element $|V_{ub}|$. We plan to return to these applications in the near future.

A Tree-level amplitudes

In this Appendix we collect formulas for helicity amplitudes for top quark decay processes $t \to b + n_g g + e^+ + \nu$, for $n_g \leq 2$. We note that we prefer to use helicity amplitudes for reasons of speed and efficiency of the computation. While for top quark decay this is not a critical issue – the number of diagrams is sufficiently small even at NNLO – it becomes essential if one considers applicability of similar techniques to more complicated processes. Some amplitudes that we present below have already appeared in the literature [7] while others are new.

To deal with the massive top quark, we follow the standard procedure that is based on the decomposition of a time-like four-momentum into a sum of two light-like four-momenta [60]. To accomplish this, we choose an arbitrary light-like momentum η and write

$$p_t = p_1 + \frac{m_t^2}{s_{p_t\eta}}\eta, \tag{A.1}$$

where $s_{ij} = 2p_i \cdot p_j$. We note that $p_1^2 = 0$ by construction. We can now write the top quark spinor as

$$
\begin{aligned}
u_-(p_t) &= (\slashed{p}_t + m_t)|\eta\rangle \frac{1}{\langle 1\eta\rangle} = |1] + |\eta\rangle \frac{m_t}{\langle 1\eta\rangle}, \\
u_+(p_t) &= (\slashed{p}_t + m_t)|\eta] \frac{1}{[1\eta]} = |1\rangle + |\eta] \frac{m_t}{[1\eta]},
\end{aligned} \tag{A.2}
$$

where we use the standard notation for spinor-helicity variables. In particular, for $p_i^2 = 0$, $|i\rangle = |p_i\rangle = u_+(p_i)$ and $|i] = |p_i] = u_-(p_i)$. It is convenient to choose the auxiliary momentum η to be the positron momentum p_6 to compute helicity amplitudes.

We now present results for helicity amplitudes starting from the tree-level process $t(p_t) \rightarrow b(p_2) + \nu(p_5) + e^+(p_6)$. We introduce the Breit-Wigner denominator $D_W(p_W^2) = (p_W^2 - m_W^2 + im_W\Gamma_W)^{-1}$ and write the amplitude as

$$\mathcal{A}_{h_t}(p_t, p_2; p_5, p_6) = g_W^2 D_W(s_{56})\delta_{i_1 i_2} A_{h_t}(1, 2; 5, 6) \equiv \mathcal{F}\delta_{i_1 i_2} A_{h_t}(1, 2; 5, 6). \tag{A.3}$$

The amplitude $A_{h_t}(1, 2; 5, 6)$ is the color-stripped amplitude and it only depends on the helicity of the top quark h_t since helicities of all massless fermions are fixed thanks to the left-handed nature of the weak current. We find

$$A_+(1, 2; 5, 6) = 0, \quad A_-(1, 2; 5, 6) = \langle 25\rangle [61]. \tag{A.4}$$

In this case the sum over colors and helicities is trivial; the amplitude squared reads

$$\sum_{\text{col,hel}} \mathcal{A}_{h_t}(p_t, p_2; p_5, p_6) = |\mathcal{F}|^2 N_c |A_-(1, 2; 5, 6)|^2. \tag{A.5}$$

Next, we consider amplitudes for the process $t(p_t) \rightarrow b(p_2) + g(p_3) + \nu(p_5) + e^+(p_6)$. We write it as

$$\mathcal{A}_{h_t h_g}(p_t, p_2, p_3; p_5, p_6) = g_s \mathcal{F} T_{i_2 i_1}^{a_3} A_{h_t h_g}(1, 2, 3; 5, 6), \tag{A.6}$$

where T^a is an $SU(3)$ color matrix normalized as $\text{Tr}(T^a T^b) = \delta^{ab}$ and $h_{t,g}$ are helicities of the top quark and of the gluon, respectively. We obtain the following results for the color-stripped helicity amplitudes

$$\begin{aligned}
A_{--}(1, 2, 3; 5, 6) &= -\frac{[61]\langle 3|\hat{p}_{56}|2]\langle 25\rangle}{\langle 3|\hat{p}_t|3][32]} - \frac{[61]\langle 35\rangle}{[32]}, \\
A_{-+}(1, 2, 3; 5, 6) &= -\frac{[61]\langle 2|\hat{p}_{56}|3]\langle 25\rangle}{\langle 3|\hat{p}_t|3]\langle 23\rangle} - \frac{[31][63]\langle 2|5\rangle}{\langle 3|\hat{p}_t|3]}, \\
A_{++}(1, 2, 3; 5, 6) &= -m_t \frac{\langle 25\rangle [63]^2}{[61]\langle 3|\hat{p}_t|3]}, \\
A_{+-} &= 0,
\end{aligned} \tag{A.7}$$

where $p_{56} = p_5 + p_6$. The sum over colors is trivial also in this case. We find

$$\sum_{\text{col}} |\mathcal{A}|^2 = |\mathcal{F}|^2 g_s^2 (N_c^2 - 1)|A|^2 = 2N_c C_F |\mathcal{F}|^2 g_s^2 |A|^2. \tag{A.8}$$

The last set of tree amplitudes that we require for our calculation are the ones that describe the process with two gluons in the final state $t(p_t) \rightarrow b(p_2) + g(p_3) + g(p_4) + \nu(p_5) + e^+(p_6)$. We write

$$\mathcal{A}_{h_t h_{g_3} h_{g_4}}(p_t, p_2, p_3, p_4; p_5, p_6) = \mathcal{F} g_s^2 \sum_\sigma (T^{a_{\sigma_3}} \cdot T^{a_{\sigma_4}})_{i_2 i_1} A_{h_t h_{g_{\sigma_3}} h_{g_{\sigma_4}}}(1, 2, \sigma(3), \sigma(4); 5, 6), \tag{A.9}$$

where σ denotes two permutations of the gluons g_3, g_4. The color-stripped helicity amplitudes are computed to be

$$A_{---} = \frac{[61]\langle 25\rangle[2|\hat{p}_t\hat{p}_{34}|2]}{\tilde{s}_{t34}[32][42][43]} - \frac{[61]\langle 4|\hat{p}_{56}|2]\langle 25\rangle\langle 3|\hat{p}_t|2]}{\tilde{s}_{t34}[32][42][3|\hat{p}_t|3\rangle}$$

$$+ \frac{[61]\langle 45\rangle\langle 3|\hat{p}_t|2]}{[32][42][3|\hat{p}_t|3\rangle} - \frac{[61]\langle 45\rangle}{[32][43]} - \frac{[61]\langle 35\rangle}{[42][43]},$$

$$A_{--+} = \langle 25\rangle\left(\frac{[61]}{[43]\langle 34\rangle}\left(-\frac{[42]\langle 23\rangle^2}{s_{234}\langle 2|4\rangle} + \frac{\langle 3|\hat{p}_t|4]^2}{\tilde{s}_{t34}\langle 3|\hat{p}_t|3]} + \frac{\langle 2|3\rangle\langle 3|\hat{p}_t|4]}{\langle 3|\hat{p}_t|3]\langle 2|4\rangle}\right)\right.$$

$$\left.+ \frac{[4|1][6|4]\langle 3|\hat{p}_t|4]}{\tilde{s}_{t34}[4|3]\langle 3|\hat{p}_t|3]}\right) - \frac{[6|1]\langle 2|3\rangle^2\langle 3|5\rangle}{s_{234}\langle 2|4\rangle\langle 3|4\rangle},$$

$$A_{-+-} = \frac{[61]\langle 25\rangle}{[43]\langle 34\rangle}\left(\frac{[32]\langle 4|\hat{p}_t|3]}{[42]\langle 3|\hat{p}_t|3]} - \frac{[32]^2\langle 24\rangle}{s_{234}[42]} + \frac{\langle 4|\hat{p}_t|3]^2}{\tilde{s}_{t34}\langle 3|\hat{p}_t|3]}\right) +$$

$$+ \frac{[61]\langle 45\rangle}{[42]\langle 34\rangle}\left(\frac{[32]\langle 24\rangle}{s_{234}} - \frac{\langle 4|\hat{p}_t|3]}{\langle 3|\hat{p}_t|3]}\right) + \frac{[63][31]\langle 25\rangle}{[43]\langle 3|\hat{p}_t|3]}\left(-\frac{\langle 4|\hat{p}_t|3]}{\tilde{s}_{t34}} - \frac{[32]}{[42]}\right) + \frac{[31][63]\langle 45\rangle}{[42]\langle 3|\hat{p}_t|3]},$$

$$A_{-++} = \frac{\langle 25\rangle}{\tilde{s}_{t34}}\left(\frac{[61]\langle 2|\hat{p}_{56}|4]\langle 4|\hat{p}_t|3]}{\langle 24\rangle\langle 34\rangle\langle 3|\hat{p}_t|3]} - \frac{[31][63]\langle 2|\hat{p}_{56}|4]}{\langle 24\rangle\langle 3|\hat{p}_t|3]} + \frac{[61]\langle 2|\hat{p}_t|3]}{\langle 24\rangle\langle 34\rangle} +$$

$$+ \frac{[41][64]\langle 4|\hat{p}_t|3]}{\langle 34\rangle\langle 3|\hat{p}_t|3]} - \frac{[31][43][64]}{\langle 3|\hat{p}_t|3]} + \frac{[31][63]\langle 23\rangle}{\langle 24\rangle\langle 34\rangle} + \frac{2[31][64]}{\langle 34\rangle}\right),$$

and

$$A_{+--} = 0,$$

$$A_{+-+} = m_t\frac{[64]^2\langle 25\rangle\langle 3|\hat{p}_t|4]}{\tilde{s}_{t34}[43][61]\langle 3|\hat{p}_t|3]},$$

$$A_{++-} = m_t\frac{[63]^2}{[61]\langle 3|\hat{p}_t|3]}\left(-\frac{\langle 25\rangle\langle 4|\hat{p}_t|3]}{\tilde{s}_{t34}[43]} + \frac{\langle 45\rangle}{[42]} - \frac{[32]\langle 25\rangle}{[42][43]}\right),$$

$$A_{+++} = m_t\frac{\langle 25\rangle}{\langle 34\rangle\langle 3|\hat{p}_t|3]}\left(\frac{[43]\langle 1|\hat{p}_{34}|6]}{\tilde{s}_{t34}} + \frac{[63]\langle 2|\hat{p}_{34}|6]}{[61]\langle 24\rangle}\right),$$

$$\text{(A.10)}$$

with $\tilde{s}_{t34} = s_{34} - s_{3t} - s_{4t}$. The color-summed amplitude now reads

$$\sum_{\text{col}}|\mathcal{A}|^2 = 4N_c|\mathcal{F}|^2 g_s^4 C_F\left[C_F\left(|A(1,2,3,4;5,6)|^2 + |A(1,2,4,3;5,6)|^2\right) + \right.$$

$$\left.+ \left(C_F - \frac{C_A}{2}\right)2\text{Re}\left[A(1,2,3,4;5,6)A^*(1,2,4,3;5,6)\right]\right]. \tag{A.11}$$

B   Calculation of one-loop integrals for the soft limit

In this Appendix, we give an example of how one-loop eikonal integrals needed for the soft current at one-loop can be computed. Consider the four-point function, defined in Eq.(4.11)

$$I_4 = \int\frac{d^dk}{i(2\pi)^d}\frac{1}{(k-p_3)^2k^2(2p_b\cdot k)(2p_t\cdot k - 2p_t\cdot p_3)}, \tag{B.1}$$

where $p_t^2 = m_t^2$, $p_b^2 = p_3^2 = 0$. We assume that each propagator contains a term $+i0$ which defines the proper analytic continuation in cases of branch cuts.

To compute I_4, we first combine k^2 and $(k - p_3)^2$ using Feynman parameters

$$\frac{1}{k^2(k-p_3)^2} = \int\limits_0^1 \frac{\mathrm{d}x}{[(k-xp_3)^2]^2}. \tag{B.2}$$

Next, we exponentiate the eikonal quark propagators introducing the integrals over "proper time"

$$\frac{1}{(2p_t \cdot k - 2p_t \cdot p_3 + i0)(2k \cdot p_b + i0)} = -\int\limits_0^\infty \mathrm{d}\tau_1 \mathrm{d}\tau_2 e^{i2k \cdot p_b \tau_1 + i(2p_t \cdot k - 2p_t \cdot p_3)\tau_2}. \tag{B.3}$$

We now combine Eqs.(B.2, B.3) and shift the loop momentum $k \to k + p_3 x$. The resulting integral becomes

$$I_4 = i \int\limits_0^\infty \mathrm{d}\tau_1 \mathrm{d}\tau_2 \int\limits_0^1 \mathrm{d}x e^{i(-2p_t \cdot p_3(1-x)\tau_2 + 2p_3 \cdot p_b x\tau_1)} \int \frac{\mathrm{d}^d k}{(2\pi)^d} \frac{1}{[k^2]^2} e^{ik(2p_t\tau_2 + 2p_b\tau_1)}. \tag{B.4}$$

The integral over k is easily evaluated

$$\int \frac{\mathrm{d}^d k}{(2\pi)^d} \frac{1}{[k^2]^2} e^{ik(2p_t\tau_2 + 2p_b\tau_1)} = \frac{i^{1+2\epsilon}\Gamma(-\epsilon)}{(4\pi)^{d/2}} [m_t^2\tau_2^2 + 2p_t \cdot p_b\tau_2\tau_1]^\epsilon. \tag{B.5}$$

To proceed further, we change variables $\tau_1 = \tau_2\xi$, $0 \le \xi \le \infty$ and integrate over τ_2 and x. We obtain

$$I_4 = -\frac{\Gamma(-\epsilon)\Gamma(1+2\epsilon)}{(4\pi)^{d/2}} \int\limits_0^\infty \frac{\mathrm{d}\xi \, (m_t^2 + 2p_t \cdot p_b\xi)^\epsilon}{(2p_t \cdot p_3 + 2p_b \cdot p_3\xi)} \left(\frac{e^{2\pi i\epsilon}}{(2p_b \cdot p_3\xi)^{1+2\epsilon}} + \frac{1}{(2p_t \cdot p_3)^{1+2\epsilon}} \right). \tag{B.6}$$

The final integration over ξ is easy to perform in terms of hypergeometric functions. The result is shown in Eq.(4.12).

References

[1] M. Jezabek and J.H. Kuhn, Nucl. Phys. B**314**, 1 (1989).

[2] A. Czarnecki, Phys. Lett. B**252**, 467 (1990).

[3] C.S. Li, R.J. Oakes and T.C. Yuan, Phys. Rev. D**43**, 3759 (1991).

[4] A. Denner and T.Sack, Nucl. Phys. B**358**, 46 (1991); G. Eliam, R. Mendel, R. Mingeron and A. Soni, Phys. Rev. Lett. **66**, 3105 (1991).

[5] J. Campbell, R. K. Ellis and F. Tramontano, Phys. Rev. D**70**, 094012 (2004).

[6] J. M. Campbell and F. Tramontano, Nucl. Phys. B**726**, 109 (2005) [hep-ph/0506289].

[7] J. M. Campbell and R. K. Ellis, arXiv:1204.1513 [hep-ph].

[8] K. Melnikov and M. Schulze, JHEP **0908**, 049 (2009) [arXiv:0907.3090 [hep-ph]].

[9] W. Bernreuther and Z. -G. Si, Nucl. Phys. B **837**, 90 (2010) [arXiv:1003.3926 [hep-ph]].

[10] K. Melnikov, M. Schulze and A. Scharf, Phys. Rev. D **83**, 074013 (2011) [arXiv:1102.1967 [hep-ph]].

[11] K. Melnikov, A. Scharf and M. Schulze, Phys. Rev. D **85**, 054002 (2012) [arXiv:1111.4991 [hep-ph]].

[12] P. Baernreuther, M. Czakon and A. Mitov, Phys. Rev. Lett. **109**, 132001 (2012) [arXiv:1204.5201 [hep-ph]].

[13] M. Czakon and A. Mitov, JHEP **1212**, 054 (2012) [arXiv:1207.0236 [hep-ph]].

[14] M. Czakon and A. Mitov, arXiv:1210.6832 [hep-ph].

[15] A. Denner, S. Dittmaier, S. Kallweit and S. Pozzorini, Phys. Rev. Lett. **106**, 052001 (2011) [arXiv:1012.3975 [hep-ph]].

[16] A. Denner, S. Dittmaier, S. Kallweit and S. Pozzorini, JHEP **1210**, 110 (2012) [arXiv:1207.5018 [hep-ph]].

[17] See contirbution by A. Denner, S. Dittmaier, S. Kallweit, S. Pozzorini and M. Schulze to J. Alcaraz Maestre *et al.* [SM AND NLO MULTILEG and SM MC Working Groups Collaboration], arXiv:1203.6803 [hep-ph], page 55.

[18] A. Czarnecki and K. Melnikov, Nucl. Phys. B**544**, 520 (1999).

[19] K. G. Chetyrkin, R. Harlander, T. Seidenstcker and M. Steinhauser, Phys. Rev. D**60**, 114015 (1999).

[20] I.R. Blokland, A. Czarnecki, M. Slusarczyk and F. Tkachov, Phys. Rev. Lett. **93**, 062001 (2004).

[21] I. Blokland, A. Czarnecki, M. Slusarczyk, F. Tkachov, Phys. Rev. D**71**, 054004 (2005) [Erratum-ibid. D**79**, 019901 (2009)].

[22] A. Czarnecki, J. G. Körner and J.H. Piclum, Phys. Rev. **D**81, 111503 (2010).

[23] J. Gao, C. S. Li and H. X. Zhu, arXiv:1210.2808 [hep-ph].

[24] C.W. Bauer, S. Fleming, D. Pirjol and I.W. Stewar, Phys. Rev. D**63**, 114020 (2001); C.W. Bauer, D. Pirjol and I.W. Stewar, Phys. Rev. D**65**, 054022 (2002); M. Beneke, A.P. Chapovsky, M. Diehl and T. Feldmann, Nucl. Phys. B **643**, 431 (2002).

[25] C.W. Bauer, Z. Ligeti and M.E. Luke, Phys. Lett. B**479**, 395 (2000).

[26] C.W. Bauer, Z. Ligeti and M.E. Luke, Phys. Rev. D**64**, 113004 (2001).

[27] P. Gambino, G. Ossola, N. Uraltsev, JHEP **0509**, 010 (2005).

[28] P. Gambino, P. Giordano, G. Ossola and N. Uraltsev, JHEP **0710**, 058 (2007).

[29] M. Czakon, Phys. Lett. B**693**, 259 (2010).

[30] M. Czakon, Nucl. Phys. B**849**, 250 (2011).

[31] T. Binoth and G. Heinrich, Nucl. Phys. B**585**, 741 (2000).

[32] T. Binoth and G. Heinrich, Nucl. Phys. B**693**, 138 (2004).

[33] C. Anastasiou, K. Melnikov and F. Petriello, Phys. Rev. D**69**, 076010 (2004).

[34] S. Frixione, Z. Kunszt and A. Signer, Nucl. Phys. B **467**, 399 (1996) [hep-ph/9512328].

[35] R. Boughezal, K. Melnikov and F. Petriello, Phys. Rev. D **85**, 034025 (2012) [arXiv:1111.7041 [hep-ph]].

[36] L. J. Dixon, In Boulder 1995, QCD and beyond 539-582 [hep-ph/9601359].

[37] R. Bonciani and A. Ferroglia, JHEP **0811**, 065 (2008).

[38] G. Bell, Nucl. Phys. B**812**, 264 (2009).

[39] H. Astarian, C. Greub and B. Pecjak, Phys. Rev. D**78**, 114028 (2008).

[40] M. Beneke, T. Huber and X.-Q. Li, Nucl. Phys. B**811**, 77 (2009).

[41] T. Huber, JHEP **0903**, 024 (2009) [arXiv:0901.2133 [hep-ph]].

[42] S. Catani and M. Grazzini, Phys. Rev. Lett. **98**, 222002 (2007) [hep-ph/0703012].

[43] S. Weinzierl, JHEP **0303**, 062 (2003) [hep-ph/0302180].

[44] G. Somogyi, P. Bolzoni and Z. Trocsanyi, Nucl. Phys. Proc. Suppl. **205-206**, 42 (2010) and references therein.

[45] M. Grazzini, JHEP **02**, 043 (2008); S. Catani, L. Cieri, G. Ferrera, D. de Florian, and M. Grazzini, Phys. Rev. Lett. **103**, 082001 (2009); G. Ferrera, M. Grazzini, and F. Tramontano, Phys. Rev. Lett. **107**, 152003 (2011); S. Catani, L. Cieri, D. de Florian, G. Ferrera, and M. Grazzini, Phys. Rev. Lett. **108**, 072001 (2012); C. Anastasiou, K. Melnikov, and F. Petriello, Phys. Rev. Lett. **93**, 262002 (2004); K. Melnikov and F. Petriello, Phys. Rev. D **74**, 114017 (2006); A. Gehrmann-De Ridder, T. Gehrmann, E. W. N. Glover, and G. Heinrich, JHEP **12**, 094 (2007); A. Gehrmann-De Ridder, T. Gehrmann, E. W. N. Glover, and G. Heinrich, Phys. Rev. Lett. **100**, 172001 (2008); S. Weinzierl, Phys. Rev. Lett. **101**, 162001 (2008) 162001.

[46] A. Gehrmann-De Ridder, T. Gehrmann and E. W. N. Glover, JHEP **0509**, 056 (2005) [hep-ph/0505111].

[47] A. Daleo, T. Gehrmann and D. Maitre, JHEP **0704**, 016 (2007) [hep-ph/0612257].

[48] C. Anastasiou, F. Herzog and A. Lazopoulos, JHEP **1103**, 038 (2011) [arXiv:1011.4867 [hep-ph]].

[49] A. Gehrmann-De Ridder, T. Gehrmann and M. Ritzmann, JHEP **1210**, 047 (2012) [arXiv:1207.5779 [hep-ph]].

[50] D. A. Kosower, P. Uwer, Nucl. Phys. B**563**, 477 (1999).

[51] J. M. Campbell and R.K. Ellis, Phys. Rev. D **62**, 114012 (2000). The MCFM program is publicly available from http://mcfm.fnal.gov.

[52] R. K. Ellis and G. Zanderighi, JHEP **0802**, 002 (2008) [arXiv:0712.1851 [hep-ph]].

[53] A. Denner, Fortschr. Phys. **41**, 307 (1993) [arXiv:0709.1075].

[54] R. Gavin, Y. Li, F. Petriello and S. Quackenbush, Comput. Phys. Commun. **182**, 2388 (2011) [arXiv:1011.3540 [hep-ph]].

[55] S. Catani and M. Grazzini, Nucl. Phys. B **570**, 287 (2000) [hep-ph/9908523].

[56] S. Catani and M. Grazzini, Nucl. Phys. B **591**, 435 (2000).

[57] I. Bierenbaum, M. Czakon and A. Mitov, Nucl. Phys. B **856**, 228 (2012) [arXiv:1107.4384 [hep-ph]].

[58] G.P. Lepage, Cornell preprint CLNS-80/447

[59] T. Hahn, Comput.Phys.Commun. **168**, 78 (2005).

[60] R. Kleiss and J. Stirling, Nucl. Phys. B**262**, 235 (1985).